α,ω-Diferrocenyl Cumulene Molecular Wires. Synthesis, Spectroscopy, Structure, and Electrochemistry

Wolfgang Skibar,[†] Holger Kopacka,[†] Klaus Wurst,[†] Christoph Salzmann,[†] Karl-Hans Ongania,[‡] Fabrizia Fabrizi de Biani,[§] Piero Zanello,*[,§] and Benno Bildstein*[,†]

Institute of General, Inorganic and Theoretical Chemistry, University of Innsbruck, Innrain 52a, 6020 Innsbruck, Austria, Institute of Organic Chemistry, University of Innsbruck, Innrain 52a, 6020 Innsbruck, Austria, and Dipartimento di Chimica, University of Siena, Via Aldo Moro, 53100 Siena, Italy

Received October 13, 2003

Cumulene sp-carbon molecular wires C_2 [Fc(Ph)C═C(Ph)Fc] up to C_7 [Fc(Ph)C═C═C═C═C═C═C(Ph)Fc] endcapped by two electroactive ferrocenyl groups are presented in this report. Synthetically, ferrocenyl cumulenes can be built-up by a modular strategy using C_1 synthon ferrocenyl(phenyl)ketone as starting material with various acetylenic/propargylic/homopropargylic C_2−C_5 reagents, taking into account and exploiting the efficient stabilization of an electron-deficient carbenium center by an adjacent ferrocenyl moiety. With increasing cumulene chain length the reactivity of cumulenes increases considerably, indicating steric protection as the main requirement for bulk stability. Even cumulenes C_2, C_4, and C_6 are conjugated "molecular wires" effecting electronic communication between the terminal ferrocenyl substituents, whereas odd cumulenes C_3, C_5, and C_7 are nonconjugated and electronically decoupled due to their orthogonal terminal π-systems. Electrochemically, separate redox waves can be detected up to a C_6 cumulene spacer, but the electronic communication between the endcapping redox-active ferrocenyl substituents decreases with increasing cumulene length.

1. Introduction

Molecular electronics[1] may be considered a combined effort from chemists and physicists to replace wires, switches, transistors, etc. of current microelectronic technology by single molecular devices, aiming ultimately at the fabrication of nanoelectronic computational appliances sometime within the next decades of this century. Our interest in this area of basic research is in the subfield of molecular wires,[2] which represent the most simple components of such future nanocircuitry. For these anticipated applications a molecular wire has to fulfill a number of criteria, inter alia (i) chemical stability, (ii) directional charge transmittal mediated through the one-dimensional molecule, (iii) modular synthetic approach to control length and dimension, and (iv) capability of interfacing with an external electric current. To address these items, we chose as model compounds rigid rods[3] made up of cumulated carbons connected to electroactive terminal ferrocenyl substituents (Chart 1, structure D). Our design principle combines the most simple and most unsaturated form of a perfectly linear carbon wire with the most convenient and most stable organometallic redox couple.[4] The endcapping ferrocenyl groups are built-in electrochemical sensors to evaluate the degree of electronic communication through the cumulene carbon wire as a function of metal-to-metal distance or length of the cumulenic bridging ligand, respectively. In comparison to *metalla*cumulenes[5] (Chart 1, structure B), which are mostly only stable in their reduced oligoyne form (Chart 1, structure C), *organic* cumulenes of type D have been known for a long time,[6] although without electroactive substituents and with a chain length of up to six cumulated carbons. In a broader context, molecular cumulenes represent low molecular

Chart 1. Design Principle of sp-Carbon Molecular Wires [M = organometallic endgroup; A, B, C, D see text]

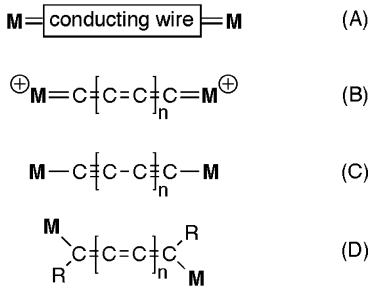

* Correspondence regarding (i) synthesis, spectroscopy, and structure (University of Innsbruck): E-mail: benno.bildstein@uibk.ac.at; (ii) electrochemistry (University of Siena): E-mail: zanello@unisi.it.
† Institute of General, Inorganic and Theoretical Chemistry, University of Innsbruck.
‡ Institute of Organic Chemistry, University of Innsbruck.
§ University of Siena.

(1) Tour, J. M. *Acc. Chem. Res.* **2000**, *33*, 791, and references therein.
(2) Reviews: (a) Astruc, D. *Acc. Chem. Res.* **1997**, *30*, 383. (b) Launay, J. P. *Chem. Soc. Rev.* **2001**, *30*, 386. (c) Ward, M. D. *Chem. Soc. Rev.* **1995**, *24*, 121. (d) Ward, M. D. *Chem. Ind.* **1996**, *15*, 568. (e) McClecverty, J. A.; Ward, M. D. *Acc. Chem. Res.* **1998**, *31*, 842. (f) Tour, J. M. *Chem. Rev.* **1996**, *96*, 537.
(3) Schwab, P. F. H.; Levin, M. D.; Michl, J. *Chem. Rev.* **1999**, *99*, 1863.
(4) Geiger, W. E. *J. Organomet. Chem. Libr.* **1990**, *22*, 142.

10.1021/om034233l CCC: $27.50
Publication on Web 01/27/2004

fragments of the hypothetical $[sp\text{-}C]_\infty$, a linear allotrope of carbon without endgroups and with all carbons connected by double (cumulene structure $=[C=C]_\infty=$) or triple bonds (polyyne structure $-[C\equiv C]_\infty-$), respectively, so-called "carbyne".[7] On the side we note that attempts to synthesize π-conjugated polymers incorporating cumulenic repeat units have been reported,[8] although the obtained polymers seem to be rather ill-defined. Cumulenic $[sp\text{-}C]_n$ systems are therefore of principal interest as possible charge carriers in comparison to other organic conductors such as polyacetylene,[9] which contains $[sp^2\text{-}C]$ repeat units. In this and in an upcoming theoretical paper, we summarize our experimental, spectroscopic, structural, electrochemical, and theoretical results on α,ω-diferrocenyl cumulenes and we compare and evaluate their performance as conducting molecular wires.

Conceptually, our design principle of cumulene molecular wires with two endcapping electroactive ferrocenyl groups consists of a modular approach that allows stepwise construction of cumulenes with an increasing number of cumulated carbons. As starting material we chose ferrocenyl(phenyl)ketone as the C_1 synthon, which contains as "innocent" spectator moiety a phenyl group; this is advantageous due to the improved stability of aryl cumulenes versus alkyl cumulenes.[6] The synthetic procedures outlined below are based on the chemistry of tetraferrocenylcumulenes, which we have investigated earlier;[10] however, for the purpose of an intended use as molecular wires these tetraferrocenyl compounds contain too many redox-active termini, which prevents evaluation of the degree of electronic communication along the cumulene bridging ligand due to interfering vicinal ferrocene−ferrocene redox couples. On the other hand, ferrocenyl(phenyl)cumulenes are structurally more complex; Chart 2 gives an overview of their essential stereochemical and configurational features.

Chart 2. Stereochemical Structures of Even/Odd Cumulenes Containing Two Pairs of Ferrocenyl/Phenyl Termini

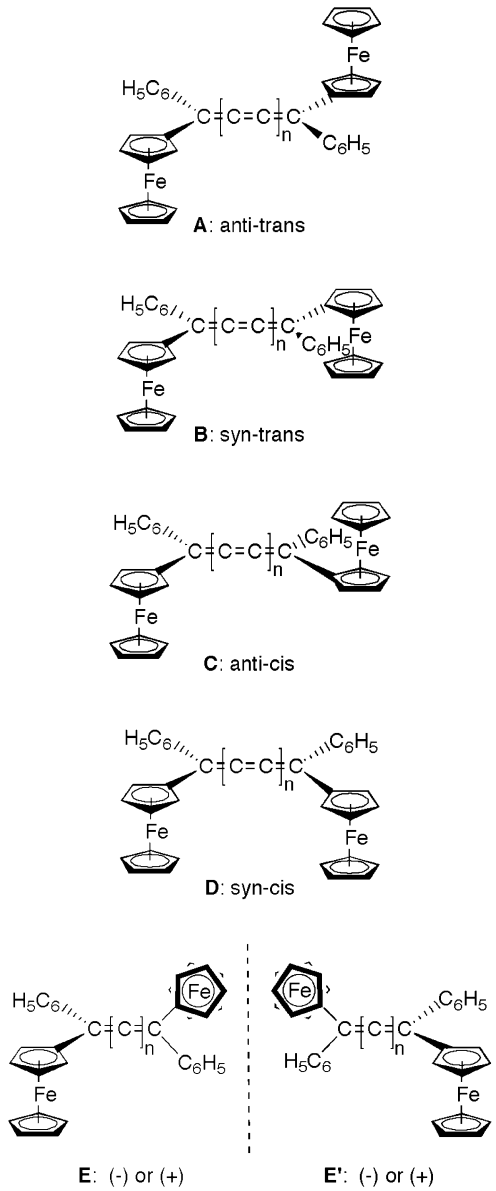

In principle, there is a significant difference between cumulenes with an even $(2n+2)$ and odd number $(2n+1)$ of carbons: even cumulenes with two different substituents are coplanar and display E/Z or cis/trans isomerism, similar to simple alkenes.[11] If there is a rotational barrier of the ferrocenyl substituents attached to the cumulene moiety, four different cis/trans/syn/anti isomers, A, B, C, and D, are possible for a $2n+2$ carbon cumulene of given connectivity (compare Chart 2). The existence or nonexistence of such diastereoisomers (especially the atropisomeric syn/anti forms) depends on steric strain, length of the cumulene, and physical state at a given temperature (vide infra). On the other hand, odd cumulenes contain a chiral axis and their two pairs of substituents are in two perpendicular planes, giving rise to enantiomerism.[12] However, the two enan-

(5) (a) Paul, F.; Lapinte, C. *Coord. Chem. Rev.* **1998**, *178−180*, 431. (b) Mohr, W.; Stahl, J.; Hampel, F.; Gladysz, J. A. *Inorg. Chem.* **2001**, *40*, 3263. (c) Meyer, W. E.; Amoroso, A. J.; Horn, C. R.; Jaeger, M.; Gladysz, J. A. *Organometallics* **2001**, *20*, 1115. (d) Paul, F.; Meyer, W. E.; Toupet, L.; Jiao, H.; Gladysz, J. A.; Lapinte, C. *J. Am. Chem. Soc.* **2000**, *122*, 9405. (e) Dembinski, R.; Bartik, T.; Bartik, B.; Jaeger, M.; Gladysz, J. A. *J. Am. Chem. Soc.* **2000**, *122*, 810. (f) Le Stang, S.; Paul, F.; Lapinte, C. *Organometallics* **2000**, *19*, 1035. (g) Ren, T.; Zou, G.; Alvarez, J. C. *Chem. Commun.* **2000**, 1197. (h) Hartbaum, C.; Mauz, E.; Roth, G.; Weissenbach, K.; Fischer, H. *Organometallics* **1999**, *18*, 2619. (i) Coat, F.; Guillemot, M.; Paul, F.; Lapinte, C. *J. Organomet. Chem.* **1999**, *578*, 76. (j) Bartik, T.; Weng, W.; Ramsden, J. A.; Szafert, S.; Falloon, S. B.; Arif, A. M.; Gladysz, J. A. *J. Am. Chem. Soc.* **1998**, *120*, 11071. (k) Brady, M.; Weng, W.; Zhou, Y.; Seyler, J. W.; Amoroso, A. J.; Arif, A. M.; Böhme, M.; Frenking, G.; Gladysz, J. A. *J. Am. Chem. Soc.* **1997**, *119*, 775. (l) Coat, F.; Guillevic, M.; Toupet, L.; Paul, F.; Lapinte, C. *Organometallics* **1997**, *16*, 5988. (m) Le Narvor, N.; Toupet, L.; Lapinte, P. *J. Am. Chem. Soc.* **1995**, *117*, 7129.

(6) (a) Fischer, H. Cumulenes. In *The Chemistry of Alkenes*; Patai, S., Ed.; Interscience/Wiley: London, 1964; p 1025, Chapter 13. (b) Hopf, H. The preparation of allenes and cumulenes. In *The Chemistry of Ketenes, Allenes, and Related Compounds*; Patai, S., Ed.; Interscience/Wiley: Chichester, 1980; Part 2, Chapter 20, p 781. (c) Hopf, H. *Classics in Hydrocarbon Chemistry*, Wiley-VCH: Weinheim, 2000; Chapter 9, p 171.

(7) (a) Gibtner, T.; Hampel, F.; Gisselbrecht, J.-P.; Hirsch, A. *Chem. Eur. J.* **2002**, *8*, 408, and references therein. (b) Lagow, R. J.; Kampa, J. J.; Wei, H.-C.; Battle, S. L.; Genge, J. W.; Laude, D. A.; Harper, C. J.; Bau, R.; Stevens, R. C.; Haw, J. F.; Munson, E. *Science* **1995**, *267*, 362. (c) Smith, P. P. K.; Buseck, P. R. *Science* **1982**, *216*, 984.

(8) (a) Kinoshita, I.; Kijima, M.; Shirakawa, H. *Macromol. Rapid Commun.* **2000**, *21*, 1205. (b) Kijima, M.; Kinoshita, I.; Shirakawa, H. *Synth. Met.* **1999**, *101*, 145. (c) Schkunov, M. N.; Meyer, R. K.; Gellermann, W.; Benner, R. E.; Vardeny, Z. V.; Lin, J. B.; Barton, T. *Synth. Met.* **1997**, *84*, 969.

(9) (a) Heeger, A. J. *Angew. Chem., Int. Ed.* **2001**, *40*, 2591. (b) MacDiarmid, A. G. *Angew. Chem., Int. Ed.* **2001**, *40*, 2581. (c) Shirakawa, H. *Angew. Chem., Int. Ed.* **2001**, *40*, 2575.

(10) Bildstein, B. *Coord. Chem. Rev.* **2000**, *206−207*, 369.

(11) Eliel, L. E.; Wilen, S. H. *Stereochemistry of Organic Compounds*; John Wiley & Sons: New York, 1994; Chapter 9, p 539.

Scheme 1. Synthesis of Olefin 2 (Fc = ferrocenyl, Ph = phenyl, •))) = ultrasound)

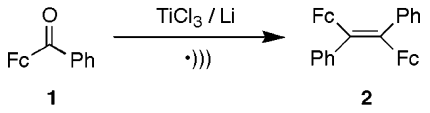

1 2

tiomers E, E′ (Chart 2) are only the residual stereoisomers that are usually encountered under normal circumstances (e.g., in solution at room temperature), but if the barrier of rotation of the ferrocenyl substituents is sufficiently high (e.g., in the solid state), three pairs of enantiomers or six different stereoisomers are possible.

The properties of even/odd cumulenes are principally different (vide infra); therefore it is quite important to distinguish between both sets of compounds. Unfortunately, the nomenclature for cumulenes stresses the number of π-bonds—rather than the number of cumulated carbons—and sometimes gives rise to misunderstandings. In general, cumulenes are defined as compounds of n carbon atoms with $(n - 1)$ double bonds connecting these n carbon atoms. Therefore cumulenes with an even number of carbons (C_4, C_6, C_8) that contain 3, 5, and 7 double bonds are referred to as [3]-, [5]-, and [7]cumulene, and cumulenes with an odd number of carbons (C_3, C_5, C_7) and with an even number of π-bonds are named as "even" [2]-, [4]-, and [6]cumulenes, respectively.

2. Results and Discussion

2.1 Synthesis, Spectroscopy, and Structure. 2.1.1. [1]Cumulene. Starting from commercially available ferrocenyl(phenyl)ketone **1**, 1,2-diferrocenyl-1,2-diphenylethylene **2** is obtained by an ultrasound-assisted reductive coupling with in situ-prepared low valent titanium (Scheme 1). These modified McMurry reaction conditions have proved essential for the synthesis of tetraferrocenylethylene[13] and are applicable in this case also, affording **2** in 23% yield (after chromatographic separation of the corresponding byproduct 1,2-diferrocenyl-1,2-diphenylethane) as an air-stable orange powder. Although **2** is a known compound[14] and by definition not a cumulene—although it may formally be considered a [1]cumulene—it is the logical starting member in our family of $Fc(C_6H_5)C_x(C_6H_5)Fc$ compounds (x = 2, 3, 4, 5, 6, 7). In solution, NMR spectroscopy indicates formation of the trans-anti isomer only (compare Chart 2), which may be rationalized by minimization of steric repulsions in this "as-short-as-possible" pseudo-cumulene. Figure 1 shows the single-crystal X-ray structure of **2**; relevant bond distances and angles are given in the figure caption. **2** exists as the trans-anti isomer A (Chart 2) with an overall strongly distorted conformation. Clearly visible is the steric strain in this molecule; most notably the phenyl substituents are tilted by 85.0(6)° with respect to the π-plane of the olefin, thereby preventing any possible conjugation between the aromatic rings and the olefinic π-bond. Similarly, the ferrocenyl groups are tilted too

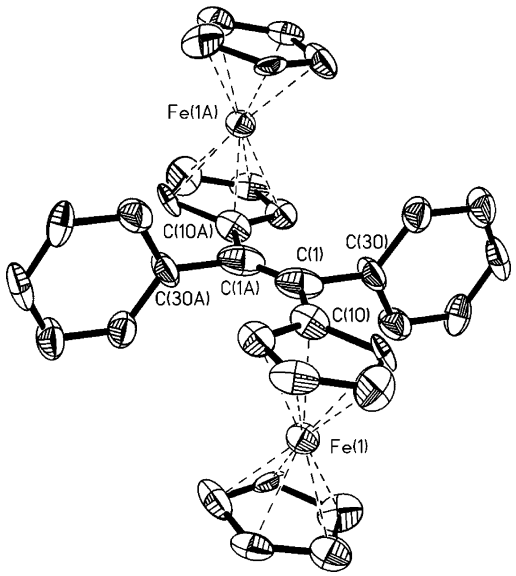

Figure 1. Molecular structure of olefin **2**, hydrogen atoms are omitted for clarity. Selected bond distances (Å) and angles (deg): C(1)−C(1A) = 1.29(4); tilt angle phenyl vs C=C plane: 85.0(6); tilt angle Cp vs C=C plane: 6.1(1.4).

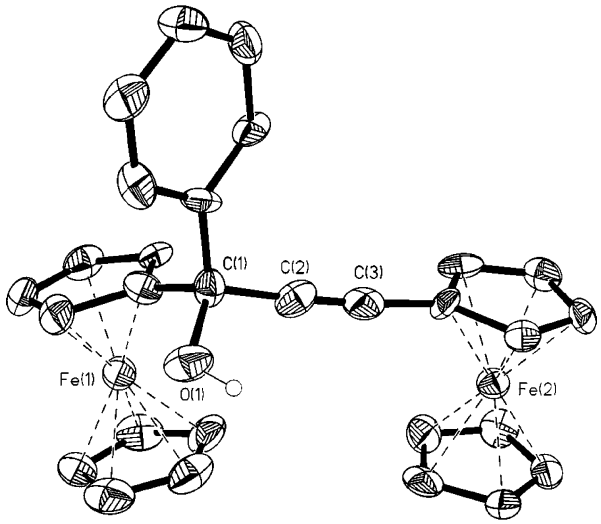

Figure 2. Molecular structure of propynol **3**, hydrogen atoms (except of hydroxyl) are omitted for clarity. Selected bond distances (Å): C(1)−C(2) = 1.468(14), C(2)−C(3) = 1.187(13), C(3)−C(20) = 1.448(14), C(1)−O(1) = 1.452(10). Selected angles (deg): C(1)−C(2)−C(3) = 177.0(13).

[6.1(1.4)° versus the C=C plane] but less so than the phenyl groups. The olefinic double bond shows a normal bond distance of 1.29(4) Å, ruling out any unusual elongation due to steric crowding. Spectroscopically, **2** is further characterized by an intense Raman vibration of the symmetrically substituted olefin ($\nu_{C=C}$ = 1572 cm^{-1}), indicative of a donor-substituted olefin, and by rather unexceptional UV−vis and NMR data (Table 1).

2.1.2. [2]Cumulene. The first true cumulene in this series of compounds is 1,2-diferrocenyl-1,2-diphenyl[2]-cumulene **5** (Scheme 2). Starting from C_1 synthon **1** the propargylic alcohol **3** can be easily prepared in 69% yield by nucleophilic addition of lithiated ferrocenylacetylene.[15] Propynol **3** is chiral and obtained as racemic mixture; Figure 2 shows its solid state structure.

(12) Eliel, L. E.; Wilen, S. H. *Stereochemistry of Organic Compounds*; John Wiley & Sons: New York, 1994; Chapter 14, p 1119.
(13) Bildstein, B.; Denifl, P.; Wurst, K.; André, M.; Baumgarten, M.; Friedrich, J.; Ellmerer-Müller, E. *Organometallics* **1995**, *14*, 4334.
(14) Dang, Y.; Geise, H.; Dommisse, R.; Esmans, E. *Inorg. Chim. Acta* **1990**, *175*, 115.
(15) Polin, J.; Schottenberger, H. *Org. Synth.* **1996**, *73*, 262.

Table 1. Key Spectroscopic and Structural Data of [2*n*+1]Cumulenes 2/11a,b/22a,b

	olefin **2** Fc(Ph)C=C(Ph)Fc	[3]cumulene **11a,b** Fc(Ph)C=C=C=C(Ph)Fc	[5]cumulene **22a,b** Fc(Ph)C=C=C=C=C=C(Ph)Fc
δ $^{13}C_{cumulene}$ [ppm]	C(1): 143.4	$C(1)_{cis}$: 119.3 $C(1)_{trans}$: 119.4 $C(2)_{cis}$: 147.1 $C(2)_{trans}$: 147.2	C(1): 122.8 C(2): 127.0 C(3): 144.1
$d_{C=C}$ [Å]	C(1)−C(1′) = 1.29(4)	C(1)−C(2) = 1.34(2) C(2)−C(3) = 1.25(2) C(3)−C(4) = 1.38(2)	not available
UV−vis [nm/log ϵ]	240/4.30 322/4.15 468/3.18	281/4.13 337/4.15 449/3.83 576/3.36	380/3.76 479/3.97 512/3.98 618/3.64
$\nu_{cumulene}$ [cm^{-1}]	1572	2024	1962

Scheme 2. Synthesis of [2]Cumulenium Tetrafluoroborate 4a,b and Its Attempted Conversion to [2]Cumulene 5

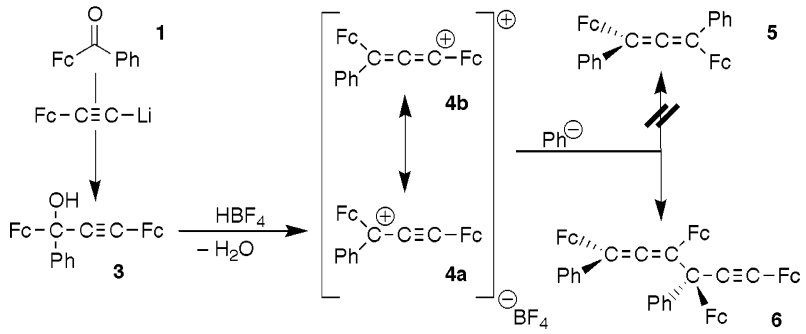

Due to the efficient stabilization of adjacent electron-deficient centers by ferrocenyl groups[16]—an essential feature[10] of the chemistry of ferrocenyl cumulenes—reaction of **3** with tetrafluoroboric acid eliminates 1 equiv of water with concomitant formation of a dark green air-stable salt **4a**,**b**. This result shows that allenylium systems with only two terminal ferrocenyl substituents are as stable as their triferrocenyl-substituted analogues, which have been prepared by us earlier.[17] The most prominent spectroscopic features of **4a**,**b** are its intense color (λ_{max} = 869 nm, log ϵ = 3.88), a very strong IR absorption in the cumulene region ($\nu_{C=C=C}$ = 2137 cm^{-1}), and three acceptor-shifted ^{13}C NMR signals for the allenylium carbons (δ = 101.4, 127.5, 143.9 ppm). To get access to 1,2-diferrocenyl-1,2-diphenyl[2]cumulene, **5**, we attempted regioselective nucleophilic addition of various metalated phenyl synthons to the ambident electrophile **4a**,**b**, but in no case was the desired cumulene formed, in contrast to tetraferrocenylallene,[17] where such a protocol has been successfully applied. Depending on solvents employed and other reaction conditions, various radical coupling products have been observed, inter alia allenalkyne **6**. Obviously **4a**,**b** is quite easily reduced to the corresponding allene radical by the phenyl nucleophile, resulting finally in single electron transfer (SET)[18] follow-up products. In addition we note that the desired [2]cumulene **5** cannot be prepared by reduction of 2,3-diferrocenyl-2,3-diphenyl-1,1-dihalocyclopropane with elemental metals, because this possible starting material for a Doering−Moore−Skattebøl allene synthesis[6b] is unfortunately unavailable from olefin **2** by reaction with dichlorocarbene, at least in our hands. However, allene **5** has been synthesized as early as 1981 by a multistep condensation/reduction/dehydration sequence in 3.6% overall yield starting from acetylferrocene and methylferrocenecarboxylate.[19] Although chromatography allowed only partial optical resolution of **5**, ^{1}H and ^{13}C NMR showed clearly the existence of only one racemic species in solution,[19] in accord with unrestricted rotation of the two pairs of ferrocenyl/phenyl groups in this shortest [2*n*+2]cumulene. For comparison with the other [2*n*+1]cumulenes discussed in this paper, the spectroscopic properties[19] of cumulene **5** [^{13}C NMR: δ C(1) = 109.2, δ C(2) = 207.1 ppm; UV−vis: $\lambda_{max(1)}$ = 450 nm, log ϵ = 2.78; $\lambda_{max(2)}$ = 340 nm, log ϵ = 3.44] are informative (compare Table 1). These key spectroscopic data of diferrocenyl(diphenyl)allene **5** are almost identical with those of tetraferrocenylallene[17] reported by us previously.

2.1.3. [3]Cumulene. For a modular synthesis of 1,4-diferrocenyl-1,4-diphenyl[3]cumulene, **11**, starting from C_1 synthon **1** a four-carbon chain has to be assembled by sequential reaction of ketone **1** with a dimetalated C_2 alkyne reagent (Scheme 3). This may be achieved by preparing trimethylsilyl-protected propynol **7** by nucleophilic addition of lithiated trimethylsilylethyne to **1**, protection of the free hydroxyl group as its methyl ether **8**, removal of the trimethylsilyl group by alkaline hydrolysis, metalating alkyne-deprotected propargylic ether **9** (Figure 3) with butyllithium, followed by nucleophilic addition to ketone **1** to afford hydroxymethoxybut-2-yne **10** (Figure 4), and finally reduction with Stephen's

(16) (a) Lukasser, J.; Angleitner, H.; Schottenberger, H.; Schweiger, M.; Bildstein, B.; Ongania, K.-H.; Wurst, K. *Organometallics* **1995**, *14*, 5566, and references therein. (b) Watts, W. E. In Wilkinson, G., Stone, F. G. A., Abel, E. W., Eds.; *Comprehensive Organometallic Chemistry*; Pergamon: Oxford, 1982; Vol. 8, Chapter 59, p 1051. (c) Watts, W. E. *J. Organomet. Chem. Libr.* **1979**, *7*, 399.

(17) Bildstein, B.; Kopacka, H.; Schweiger, M.; Ellmerer-Müller, E.; Ongania, K.-H.; Wurst, K. *Organometallics* **1996**, *15*, 4398.

(18) (a) Savéant, J. *Adv. Phys. Org. Chem.* **1990**, *26*, 1. (b) Ashby, E. C. A. *Acc. Chem. Res.* **1988**, *21*, 414.

(19) Schlögl, K.; Widhalm, M. *Monatsh. Chem.* **1981**, *112*, 91.

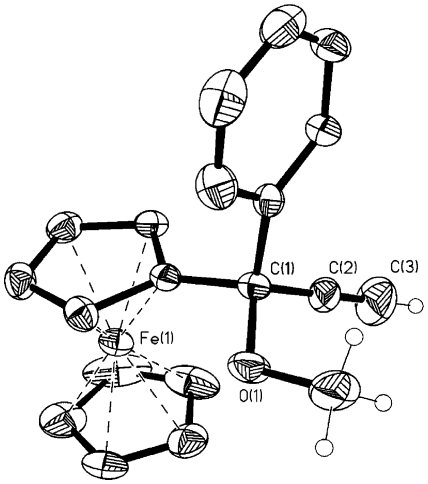

Figure 3. Molecular structure of propargyl ether **9**, hydrogen atoms (except of methoxy and alkynyl) are omitted for clarity. Selected bond distances (Å): C(1)−C(2) = 1.477(3), C(2)−C(3) = 1.163(4), C(1)−O(1) = 1.429(3), O(1)−C(4) = 1.427(3). Selected angles (deg): C(1)−C(2)−C(3) = 179.7(4).

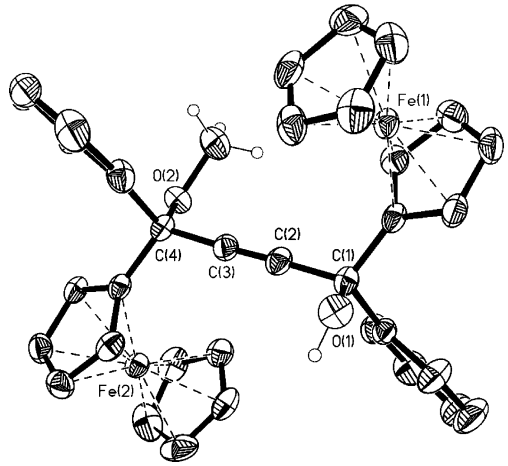

Figure 4. Molecular structure of hydroxymethoxybutyne **10**, hydrogen atoms (except of methoxy and hydroxyl) are omitted for clarity. Selected bond distances (Å): C(1)−C(2) = 1.484(4), C(2)−C(3) = 1.190(4), C(3)−C(4) = 1.491(4), C(1)−O(1) = 1.432(3), C(4)−O(2) = 1.428(3), O(2)−C(5) = 1.414(4). Selected angles (deg): C(1)−C(2)−C(3) = 177.9(3), C(2)−C(3)−C(4) = 177.3(3).

reagent ($SnCl_2$ in acetic acid)[20] to the target [3]cumulene **11a**,**b**. Overall, the yield of cumulene **11a**,**b** by this multistep sequence is 8%; the most difficult reaction is the selective reduction of precursor **10** by reducing conditions, preventing overreduction to the byproduct 1,4-diferrocenyl-1,4-diphenylbuta-1,3-diene, **12a**,**b**. Similar difficulties in chemoselectivity have been observed earlier in the analogous preparation of tetraferrocenyl-[3]cumulene.[21]

Compound **11** is obtained as a 1:1 mixture of cis and trans diastereoisomers **11a** and **11b** which proved unseparable by chromatographic methods. According to ^{1}H and ^{13}C NMR measurements at room temperature only two magnetically nonisochronous ferrocenyl/phenyl groups are observed in addition to two sets of ^{13}C signals

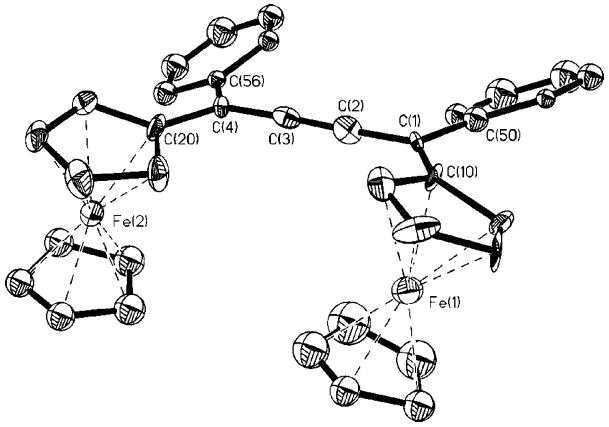

Figure 5. Molecular structure of [3]cumulene **11b**, hydrogen atoms are omitted for clarity. Selected bond distances (Å): C(1)−C(2) = 1.34(2), C(2)−C(3) = 1.25(2), C(3)−C(4) = 1.38(2). Selected angles (deg): C(1)−C(2)−C(3) = 175.9(12), C(2)−C(3)−C(4) = 178.1(12); tilt angle plane of ferrocene Fe(1) vs cumulene π-plane: 22.3(7); tilt angle plane of ferrocene Fe(2) vs cumulene π-plane: 17.7(8); tilt angle plane of phenyl C(50) vs cumulene π-plane: 27.2(6); tilt angle plane of phenyl C(56) vs cumulene π-plane: 27.3(5).

for the cumulene carbons [δ C(1)$_{cis}$ = 119.3; δ C(1)$_{trans}$ = 119.4; δ C(2)$_{cis}$ = 147.1; δ C(2)$_{trans}$ = 147.2], corresponding to cis/trans isomers **11a** and **11b** in solution, but no syn/anti isomers (compare Chart 2) are detectable, indicative of low rotational barriers of the terminal ferrocenyl/phenyl substituents. However, selective crystallization affords single crystals of solely cis **11b** in its syn conformation (Figure 5). Interestingly, for tetraferrocenyl-[3]cumulene also only the syn conformer has been found by synchrotron powder diffraction analysis,[22] suggesting that ferrocenyl[3]cumulenes in their syn conformation have better packing forces in the solid state than their anti isomers. In comparison to the crystal structure of olefin **2** (Figure 1) the two pairs of terminal ferrocenyl/phenyl substituents are farther apart due to the longer cumulene spacer and consequently no unusual steric strain is observed in [3]cumulene **11b**. Both phenyl groups are tilted by 27° with respect to the four-carbon [3]cumulene π-system, whereas the two ferrocenyl groups are tilted by 17.7° and 22.3° in relation to the cumulene π-plane, as is commonly observed for conjugated ferrocene compounds in the crystalline state. Beyond these conformational solid state properties of cumulene **11b**, the most important structural aspect is the marked bond distance alteration of the cumulene moiety: the central C═C bond [C(2)−C(3) = 1.25(2) Å] is significantly shorter than both terminal C═C bonds [C(1)−C(2) = 1.34(2) Å, C(3)−C(4) = 1.38(2) Å], indicative of electronically different bonding situations. We will address this issue in an upcoming theoretical paper, but we note at this point that early structural investigations on organic cumulenes[23] have interpreted this finding for [2*n*+1]cumulenes in terms of a contribution of ylidic resonance structures with terminal single and central triple bonds. Further characteristic spectroscopic

(20) Kuhn, R.; Krauch, H. *Chem. Ber.* **1955**, *88*, 309.
(21) Bildstein, B.; Schweiger, M.; Kopacka, H.; Wurst, K. *J. Organomet. Chem.* **1998**, *553*, 73.
(22) Dinnebier, R. E.; Schweiger, M.; Bildstein, B.; Shankland, K.; David, W. I. F.; Jobst, A.; van Smaalen, S. *J. Appl. Crystallogr.* **2000**, *33*, 1199.
(23) Irngartinger, H.; Götzmann, W. *Angew. Chem.* **1986**, *98*, 359; *Angew. Chem., Int. Ed. Engl.* **1986**, *25*, 340.

Scheme 3. Synthesis of [3]Cumulene 11a,b

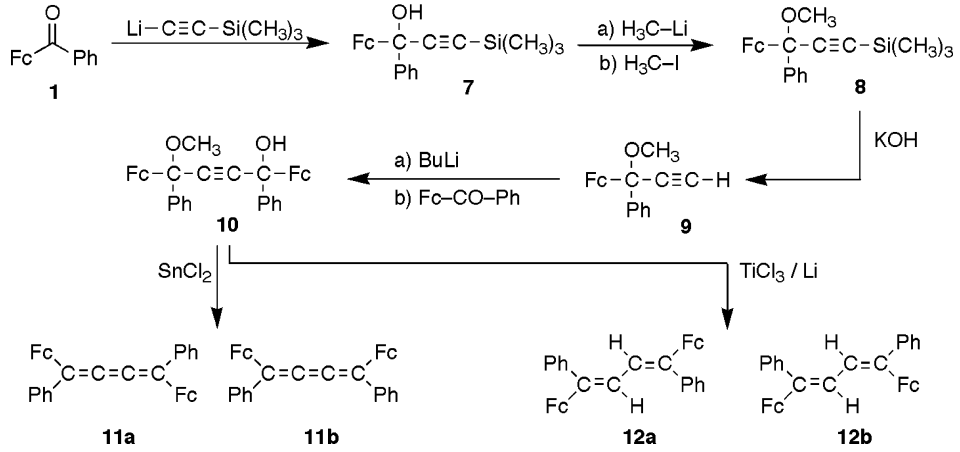

Scheme 4. Synthesis of [4]Cumulene 18

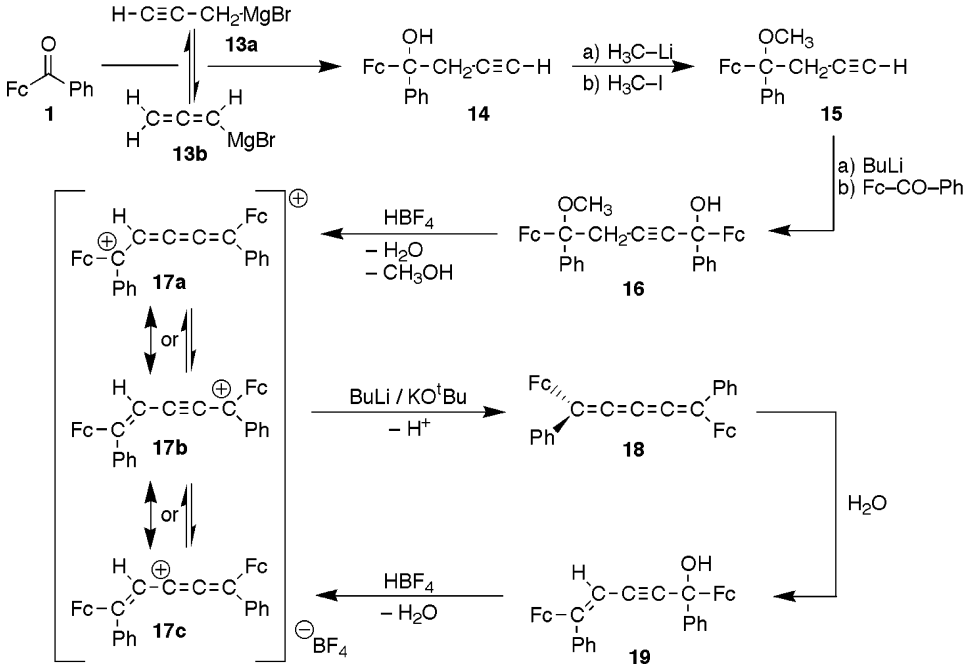

properties of [3]cumulene **11a**,**b** are an intense Raman band of the symmetric cumulene ($\nu_{C=C=C=C}$ = 2024 cm^{-1}) and two absorptions in the visible range ($\lambda_{max(1)}$ = 576 nm, log ϵ = 3.36; $\lambda_{max(2)}$ = 449 nm, log ϵ = 3.83), in accord with its red color (Table 1).

2.1.4. [4]Cumulene. The synthesis of [2*n*+2]cumulenes containing an odd number of cumulated carbons is in general much more demanding than the preparation of [2*n*+1]cumulenes,[6] mostly due to the fact that no simple C_2 acetylenic building blocks can be used for the construction of the odd-numbered cumulene carbon chain or its precursors, respectively. Nevertheless, a strategy devised previously for the case of tetraferrocenyl-[4]cumulene[24] employing a metalated C_3 building block proved successful (Scheme 4): (i) ketone **1** is reacted with a propargyl/allenyl Grignard reagent[25] **13a**,**b** to yield butynol **14** (Figure 6), (ii) the hydroxy group of **14** is protected as its methyl ether by sequential reaction with methyllithium and methyl iodide, (iii) deprotonation of **15** followed by nucleophilic addition to ketone **1** affords methoxypentynol **16**, and (iv) reaction of precursor **16** with 1 equiv of tetrafluoroboric acid eliminates simultaneously water and methanol to give the purple protonated [4]cumulenium salt **17a**,**b**,**c** in excellent 46.6% overall yield. The last step of this unusual sequence deserves some comments: the terminal ferrocenyl substituents serve as α-carbenium stabilizing groups,[16] which facilitate removal of an α-nucleofuge (e.g., methoxide or hydroxide) by protonation with a sufficiently strong acid which has a nonnucleophilic anion or conjugate base, respectively. This chemistry was planned in the design of our synthetic route, but it is quite unexpected and most unusual that only one proton effects removal of both water and methanol in a single step, feasible because of the high degree of conjugation in this unique cumulene salt and due to the acidifying effect of a positively charged carbenium center on a neighboring CH_2 group that is part of a propargyl moiety. Spectroscopically, cumulenium salt **17a**,**b**,**c** is characterized by a very strong IR absorption ($\nu_{C=C=C=CH-C}$ = 2101 cm^{-1}) and by an intense charge transfer band (λ_{max} = 941 nm, log ϵ = 4.03), similar to other organometallic near-infrared absorbing dyes.[26] The ^1H and ^{13}C NMR signal sets suggest that cumulenium salt **17** is a resonance hybrid of the contributing Lewis structures **17a**,**b**,**c**, but an equilibrium between

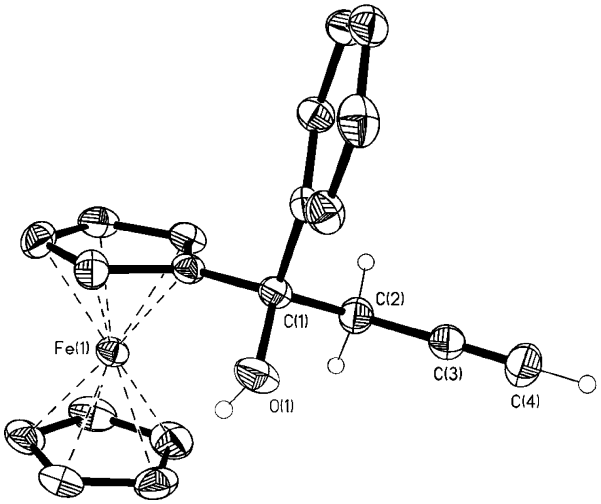

Figure 6. Molecular structure of butynol **14**, hydrogen atoms of ferrocenyl and phenyl are omitted for clarity. Selected bond distances (Å): C(1)−C(2) = 1.547(2), C(2)−C(3) = 1.463(2), C(3)−C(4) = 1.168(2), C(1)−O(1) = 1.4261(19). Selected angles (deg): C(1)−C(2)−C(3) = 113.55(14), C(2)−C(3)−C(4) = 178.0(2).

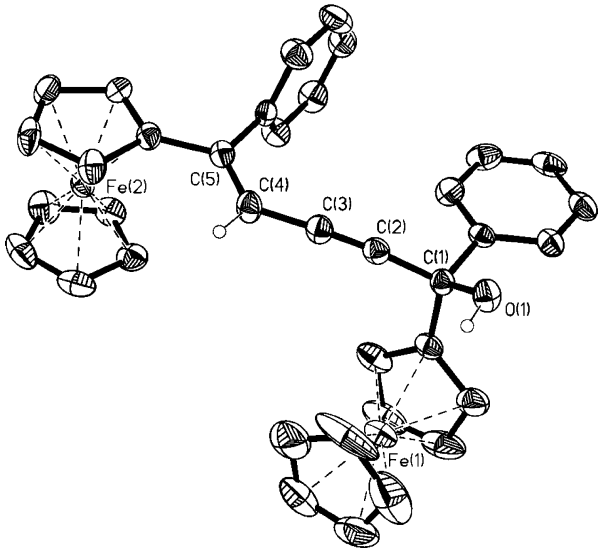

Figure 7. Molecular structure of pentenynol **19**, hydrogen atoms of ferrocenyl and phenyl are omitted for clarity. Selected bond distances (Å): C(1)−C(2) = 1.477(3), C(2)−C(3) = 1.194(3), C(3)−C(4) = 1.425(3), C(4)−C(5) = 1.338(3), C(1)−O(1) = 1.436(3). Selected angles (deg): C(1)−C(2)−C(3) = 174.8(2), C(2)−C(3)−C(4) = 176.6(3), C(3)−C(4)−C(5) = 124.1(2).

distinct compounds **17a**, **17b**, and **17c** cannot be ruled out, due to overlapping signals and difficulties in assignments for the quaternary carbons of the cationic cumulene moiety. This is a general problem in such cumulenium salts (vide infra), indicated by both "resonance" and "equilibrium" arrows in Scheme 4.

From a preparative viewpoint, this unusual compound is nothing else than the conjugate acid of 1,5-diferrocenyl-1,5-diphenyl[4]cumulene, **18**; therefore a suitable base should allow its synthesis. Indeed, "superbases" or "Schlosser bases" (equimolar mixtures of potassium alkoxides with butyllithium)[27] deprotonate a purple solution of **17a**,**b**,**c** under color change to give a red solution of cumulene **18**, similar to that in the case of tetraferrocenyl[4]cumulene.[24] However, compound **18**, containing two ferrocenyl and two phenyl termini, is sterically less protected than its tetraferrocenyl analogue, and on attempted chromatographic workup hydrolysis proved unavoidable, affording pent-4-en-2-yn-1-ol **19** (Figure 7) as the sole isolable product. Interestingly, treatment with tetrafluoroboric acid regenerates the starting material **17a**,**b**,**c** as outlined in Scheme 4.

2.1.5. [5]Cumulene. In general, C_6 cumulenes are comparatively easy to synthesize[6] because they can be obtained either by symmetrical coupling of two simple propargylic C_3 synthons[28] or by reduction of hexadiynediols,[29] which are readily accessible[30] (Scheme 5).

Deprotonation of O-protected ferrocenyl(phenyl)methoxypropyne **9** affords metalated **20**, which is stable in solution at room temperature. Upon refluxing a red THF solution of **20**, an intramolecular elimination of lithium methoxide takes place under formation of zwitterion **21b** or ferrocenyl(phenyl)ethenylidenecarbene **21a**, respectively, as an unstable intermediate,[28] which formally dimerizes to 1,6-diferrocenyl-1,6-diphenyl[5]cumulene, **22a**,**b**. In comparison to tetraferrocenyl[5]cumulene,[31] where this reaction occurs at temperatures below 0 °C, much higher temperatures and extended reaction periods (ca. 12 h) are necessary for this elimination, due to the reduced stabilization of the positive charge of zwitterion **21b** by only one adjacent ferrocenyl group. Cumulene **22a**,**b** is unfortunately not as stable as tetraferrocenyl[5]cumulene,[31] most likely because of less steric protection. During the course of formation by elimination of methoxide from precursor **20** in refluxing THF, we observe partial decomposition to a black and insoluble polymer, even before all of the starting material is consumed. Therefore the yield of **22a**,**b** is quite low, only 5.6% after chromatography. On the side we note that use of other solvents and application of other sources of activation, e.g., ultrasound, were unsuccessful. In analogy to cycloaddition reactions of other organic [5]cumulenes[32] one might expect the thermal formation of [4]radialenes[33] from **22a**,**b** by [2+2]cycloaddition at the central C═C bond of cumulene **22a**,**b**, but no such radialene could be detected in our

(24) Bildstein, B.; Schweiger, M.; Kopacka, H.; Ongania, K.-H.; Wurst, K. *Organometallics* **1998**, *17*, 2414.
(25) Brandsma, L. *Preparative Acetylenic Chemistry*, 2nd ed.; Elsevier: Amsterdam, 1988; p 35.
(26) (a) Barlow, S.; Bunting, H. E.; Ringham, C.; Green, J. C.; Bublitz, G. U.; Boxer, S. G.; Perry, J. W.; Marder, S. R. *J. Am. Chem. Soc.* **1999**, *121*, 3715. (b) Wu, I.-Y.; Lin, J. T.; Wen, Y. S. *Organometallics* **1999**, *18*, 320.
(27) (a) Schlosser, M. *Mod. Synth. Methods* **1992**, *6*, 227. (b) Schlosser, M. *Pure Appl. Chem.* **1988**, *60*, 1627. (c) Caubere, P. *Chem. Rev.* **1993**, *93*, 2317.
(28) (a) Hartzler, H. D. *J. Am. Chem. Soc.* **1961**, *83*, 4990. (b) Basak, S.; Srivastava, S.; le Noble, W. J. J. *Org. Chem.* **1987**, *52*, 5095.
(29) (a) Kuhn, R.; Wallenfels, K. *Ber. Dtsch. Chem. Ges.* **1938**, *71*, 1510. (b) Kuhn, R.; Krauch, H. *Chem. Ber.* **1955**, *88*, 309. (c) Ried, W.; Schlegelmilch, W.; Piesch, S. *Chem. Ber.* **1963**, *96*, 1221.
(30) Brandsma, L.; Vasilevsky, S. F.; Verkruijsse, H. D. *Application of Transition Metal Catalysts in Organic Synthesis*; Springer-Verlag: Berlin, 1988.
(31) Bildstein, B.; Schweiger, M.; Angleitner, H.; Kopacka, H.; Wurst, K.; Ongania, K.-H.; Fontani, M.; Zanello, P. *Organometallics* **1999**, *18*, 4286.
(32) Kaftory, M.; Agmon, I.; Ladika, M.; Stang, P. J. *J. Am. Chem. Soc.* **1987**, *109*, 782.
(33) (a) Hopf, H.; Maas, G. *Angew. Chem.* **1992**, *104*, 953; *Angew. Chem., Int. Ed. Engl.* **1992**, *31*, 931. (b) Hopf, H. *Classics in Hydrocarbon Chemistry*; Wiley-VCH: Weinheim, 2000; Chapter 11, p 290.

Scheme 5. Synthesis of [5]Cumulene 22a,b

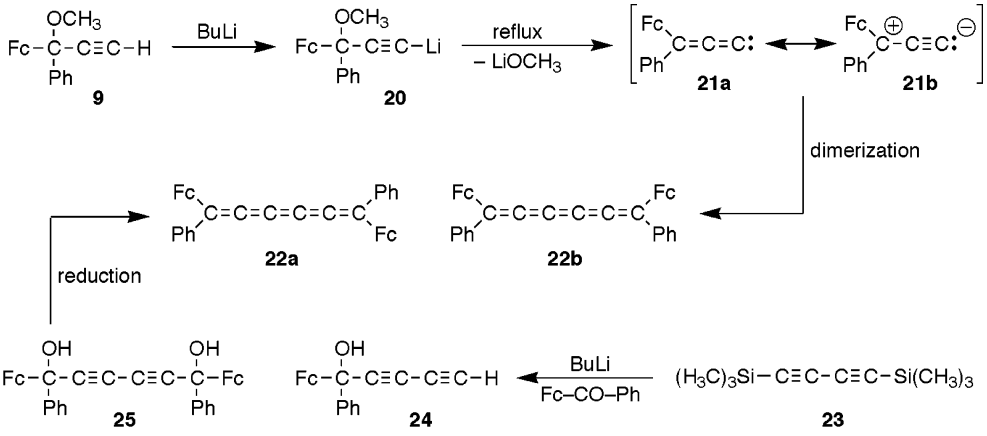

Scheme 6. Synthesis of [6]Cumulenium Tetrafluoroborate 29a,b,c,d and Its Attempted Deprotonation to [6]Cumulene 30

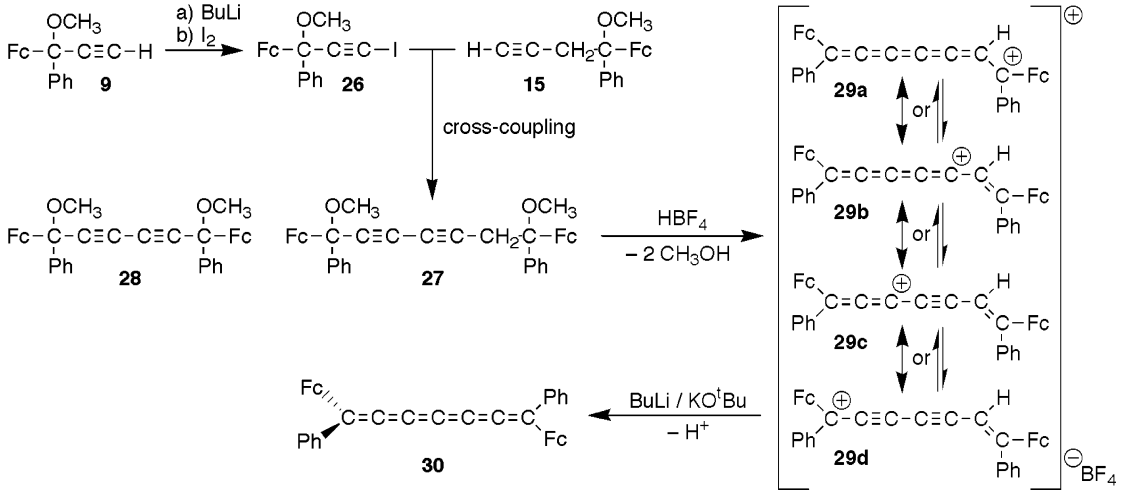

case; only a polymeric black tar was observed. As an alternative synthetic route to cumulene **22a**,**b**, bis(trimethylsilyl)butadiyne **23** was metalated and converted to pentadiynol **24** and hexabutadiynediol **25** in one step. Reduction of **25** with stannous chloride[29] does afford cumulene **22a**,**b** according to TLC analysis, but attempted workup of the reaction mixture failed to give any isolated product.

1,6-Diferrocenyl-1,6-diphenyl[5]cumulene, **22a**,**b**, is obtained as a moderately air-stable powder (mp 244 °C, dec) of purple color ($\lambda_{max} = 618$ nm, $\log \epsilon = 3.64$). Figure 8 shows the UV−vis spectra of [1]-, [3]-, [5]cumulenes **2**, **11a**,**b**, and **22a**,**b** in comparison; one can clearly see the expected bathochromic shift and increasing molar extinction coefficient with increasing chain length of the cumulene. The symmetric cumulene moiety of **22a**,**b** is characterized by an intense Raman band ($\nu_{C=C=C=C=C=C} = 1962$ cm^{-1}) at lower energy than in C_4 cumulene **11a**,**b** (Table 1). ^{1}H and ^{13}C NMR spectroscopy reveals only one set of signals for the ferrocenyl and phenyl groups, and only three cumulene carbons [δ C(1) = 122.8, δ C(2) = 127.0, δ C(3) = 144.1 ppm] are detected; therefore all four possible isomers (syn/anti and cis/trans, compare Chart 2) are in equilibrium in solution due to low rotational barrier of the ferrocenyl substituents and due to facile cis/trans isomerization. Obviously the activation energy of cis/trans isomerization for [2*n*+1]cumulenes decreases with increasing chain length, as one might expect; we will deal with this stereochemical aspect in a theoretical paper in preparation. On the side we note that there is only one single report in the literature of cis/trans isomers of a [5]cumulene in solution with an estimated activation enthalpy of 20 kcal/mol.[34] Probably due to the fluctuating structure of cumulene **22a**,**b**, it was not possible to grow suitable crystals for an X-ray solid state structure, despite many attempts.

2.1.6. [6]Cumulene. All organic cumulenes containing more than six cumulated carbons have been reported to be intractable as pure solids;[6] therefore it is quite challenging to synthesize cumulenes beyond this stability threshold. Even tetraferrocenyl[6]cumulene[35] (which is the first characterized C_7 cumulene) is stable only in solution and too reactive to be isolated. However, a [6]cumulene with just two ferrocenyl termini might be isolable due to a less nucleophilic cumulene moiety substituted by only two ferrocenyl donor groups. Therefore we set out to prepare 1,7-diferrocenyl-1,7-diphenyl-[6]cumulene by a synthetic strategy similar to the preparation of [4]cumulenes, but with an additional acetylenic C_2 synthon for the assembly of the C_7 cumulene unit (Scheme 6).

(34) Kuhn, R.; Schulz, B.; Jochims, J. C. *Angew. Chem.* **1966**, *78*, 449.

(35) Bildstein, B.; Skibar, W.; Schweiger, M.; Kopacka, H.; Wurst, K. *J. Organomet. Chem.* **2001**, *622*, 135.

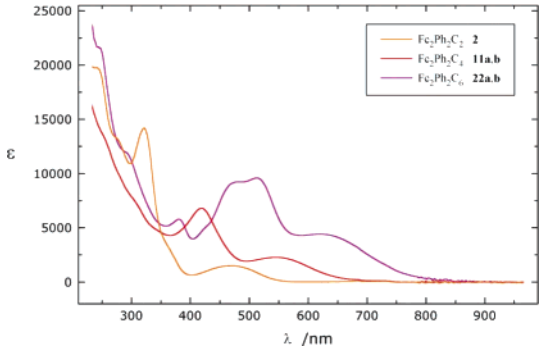

Figure 8. UV−vis spectra of [1]-, [3]-, and [5]cumulenes **2**, **11a**,**b**, and **22a**,**b**.

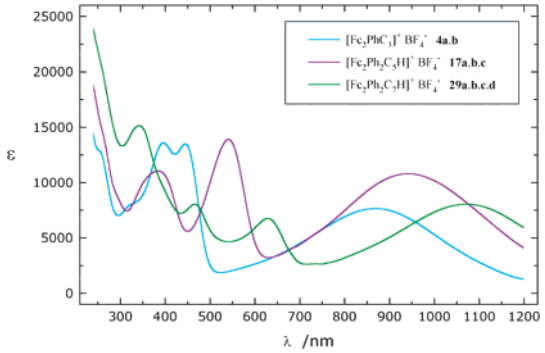

Figure 9. UV−vis−NIR spectra of [2]-, [4]-, and [6]-cumulenium salts **4a**,**b**, **17a**,**b**,**c**, and **29a**,**b**,**c**,**d**.

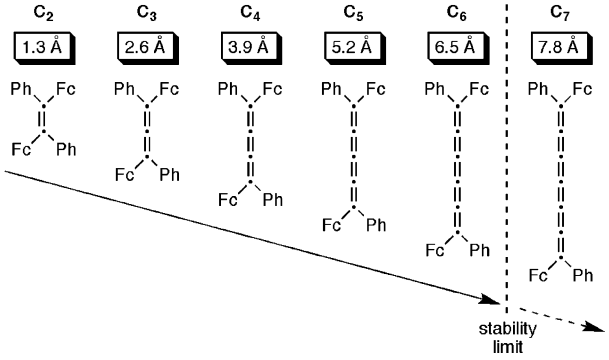

Figure 10. Comparison of [*n*]cumulenes ($n = 1-6$) synthesized. Distances [Å] refer to the length of the cumulene carbon chain.

Propargyl ether **9** is first converted to its iodo-alkyne derivative **26** and then cross-coupled with the homopropargylic ether **15** by a Cadiot−Chotkiewicz protocol[30,36] to C_7 precursor dimethoxyheptadiyne **27**, as a commonly observed byproduct in such cross-coupling reactions; also the homo-coupled dimethoxyhexadiyne **28** is obtained. Analogously as in the case of [4]cumulene **18**, addition of *1 equiv* of tetrafluoroboric acid causes *2-fold* elimination of methanol, yielding the unusual cumulenium salt **29a**,**b**,**c**,**d** as an air-sensitive dark green powder in 15.2% overall yield starting from **9**. The chemical stability of **29a**,**b**,**c**,**d** is much inferior compared to its shorter homologue **17a**,**b**,**c**, as evidenced by its sensitivity to air and by ^{1}H and ^{13}C signals that are very broad and noninformative, either due to equilibria between possible structures **29a**, **29b**, **29c**, and **29d** or due to intramolecular redox reactions, e.g., partial oxidation of a ferrocene group with concomitant partial reduction of the cationic cumulene moiety (such redox tautomerism[37] has been observed in other ferrocenyl-stablized carbenium salts). However, the identity of **29a**,**b**,**c**,**d** is corroborated by detection of the molecular ion of the cation in the positive mode FAB spectrum and from observation of an extremely strong cumulene IR absorption ($\nu_{C=C=C=C=C=CH-C} = 2049$ cm^{-1}), lower in energy than the cumulene band of the shorter homologue **17a**,**b**,**c** ($\nu_{C=C=C=C=CH-C} = 2101$ cm^{-1}), and from an intense NIR charge transfer absorption ($\lambda_{max} = 1072$ nm, $\log \epsilon = 3.91$), bathochromically shifted as compared to the corresponding band of the C_5 homologue **17a**,**b**,**c** ($\lambda_{max} = 941$ nm, $\log \epsilon = 4.03$). Figure 9 shows the UV−vis−NIR spectra of cumulenium salts **4a**,**b**, **17a**,**b**,**c**, and **29a**,**b**,**c**,**d**, respectively. As anticipated, with increasing length of the cumulene system a bathochromic shift is observed in these organometallic/cumulenic NIR dyes. Structurally, **29a**,**b**,**c**,**d** may be described by the four formulas depicted in Scheme 6 with the positive charge at the C(1), C(3), C(5), and C(7) carbon, respectively. However, vinyl-type cations **29b** and **29c** are certainly less stable than α-ferrocenyl carbenium ions **29a** and **29d**, but it is quite recognizable that a highly conjugated cumulenic unsaturated system is present, either in equilibrium or with different resonance contributions of the four possible structures.

From a chemical viewpoint, **29a**,**b**,**c**,**d** is the conjugate acid of 1,7-diferrocenyl-1,7-diphenyl[6]cumulene, **30**, and indeed it is possible to effect deprotonation of cumulenium salt **29a**,**b**,**c**,**d** by "superbase"[27] potassium *tert*-butoxide/*n*-butyllithium under formation of a burgundy red solution of neutral [6]cumulene **30**. However, much to our frustration, all our efforts to isolate this compound under a variety of experimental conditions met with failure; only unidentified decomposition products were observed. This unfortunate result shows that contrary to our expectations a C_7 cumulene with only two ferrocene termini is not stabilized against its tetraferrocenyl-substituted analogue, suggesting that steric protection is the main stabilizing factor for very long cumulenes.

2.1.7. Summary of Synthetic Cumulene Chemistry. We have developed preparative routes to cumulenes containing two electroactive ferrocenyl termini and two phenyl groups with a chain length of up to seven carbons. Our modular synthetic strategy allows a stepwise preparation of such cumulenes with various propargylic and homopropargylic building blocks, starting from ferrocenyl(phenyl)ketone as the C_1 synthon. Not only are the ferrocenyl substituents necessary electroactive components of the target cumulenes, but they also take part in the synthetic routes as potent carbenium stabilizing moieties and allow thereby access to very unusual cumulated compounds. [2*n*+1]Cumulenes (C_2, C_4, C_6) have been prepared and isolated, but [2*n*+2]-cumulenes (C_5, C_7) can be obtained in their protonated form only, not as the free neutral cumulenes. Steric protection seems to be the decisive criterion for the existence of a cumulene. Figure 10 summarizes these synthetic results and gives an overview of the length of the [1]- to [6]cumulenes synthesized in this work.

(36) Siemsen, P.; Livingston, R. C.; Diederich, F. *Angew. Chem.* **2000**, *112*, 2740; *Angew. Chem., Int. Ed.* **2000**, *39*, 2632.
(37) Bildstein, B.; Hradsky, A.; Kopacka, H.; Malleier, R.; Ongania, K.-H. *J. Organomet. Chem.* **1997**, *540*, 127, and references therein.

2.2. Electrochemistry. For the experimental evaluation of a molecular wire as a device that allows exchange of an electron or hole between its terminal redox centers, there are in principle four different methods available: measurement of the (i) bulk conductivity, (ii) conductivity of a single molecule, (iii) intervalence transition by NIR spectroscopy, and (iv) electronic interaction by cyclic voltammetry. The first approach is highly dependent on the actual solid state structure of the material and gives only a statistical figure of merit, which is dominated by intermolecular and not necessarily by intramolecular interactions. The second method would be the most accurate test, but the experimental setup is quite difficult (measurement of the current/voltage response of a single molecule inserted between an electrode and a STM tip) and has been realized only for very few systems.[38] The third method gives the electron coupling as a function of the energy and half-width of the optical intervalence transition in weakly coupled systems, but often it is difficult to deconvolute the spectra due to very broad signals and/or overlapping metal-to-ligand charge transfer bands. The fourth approach is the most convenient and the commonly used practice. It allows an indirect measurement of the "electronic communication" between the redox termini of a molecule in solution and has been applied to many intramolecular electron transfer systems. Historically the most important example is the Creutz−Taube complex.[39] In the field of molecular wires, electrochemical investigation of long-distance intervalence electron transfer has been shown to reach a detection limit at a metal-to-metal distance of approximately 25 Å, irrespective of the type of endcapping metal moiety and regardless of the type of conjugating bridging ligand.[40] One of the main questions to be answered by the work reported in this paper is "how do cumulene molecular wires perform in comparison to other systems?" To address this issue, cyclic voltammetric studies of the α,ω-diferrocenylcumulenes were performed.

2.2.1. [1]Cumulene. Olefin **2** displays two separated ferrocene-centered chemically reversible oxidations followed by an irreversible olefin-centered oxidation (Figure 11). Although the observation of two separated redox processes is not unexpected at all, the result is in accordance with our design principle of [*n*]cumulene molecular wires containing two terminal redox-active ferrocene termini which are conjugatively bridged by an unsaturated carbon spacer. Step-by-step controlled potential experiments prove the complete chemical reversibility of the redox processes $\mathbf{2}/\mathbf{2}^{+}/\mathbf{2}^{2+}$ also in the long term of macroelectrolysis. As a consequence of the first one-electron oxidation ($E_w = +0.4$ V), the original orange solution ($\lambda_{max} = 460$ nm) turns green ($\lambda_{max} = 580$ nm); upon the subsequent one-electron removal ($E_w = +0.8$ V), the solution changes slightly its tonality of green color ($\lambda_{max} = 700$ nm), indicative of the existence of two communicating chromophores [Fc(1)$^+$ and Fc(2)$^+$] in $\mathbf{2}^{2+}$.

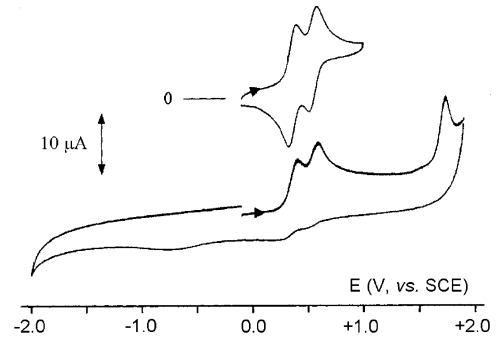

Figure 11. Cyclic voltammograms recorded at a platinum electrode in a CH_2Cl_2 solution containing **2** (0.6×10^{-3} mol/L) and $[NBu_4][PF_6]$ (0.2 mol/L). Scan rate 0.2 V s^{-1}.

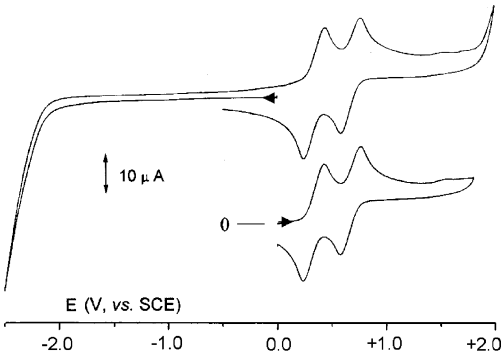

Figure 12. Cyclic voltammograms recorded at a platinum electrode in a CH_2Cl_2 solution containing **2** (0.5×10^{-3} mol/L) and $[NBu_4][B(C_6F_5)_4]$ (0.1 mol/L). Scan rate 0.2 V s^{-1}.

Changing the supporting electrolyte from $[NBu_4][PF_6]$ to $[NBu_4][B(C_6F_5)_4]$ improves the separation of the two ferrocenyl oxidations and also shifts the ethene oxidation beyond the anodic solvent discharge (Figure 12), due to the lower ion pairing of the large and weakly coordinating tetrakis(pentafluorophenyl)borate counterion.[41] However, the different half-wave peak separations of $\mathbf{2}/\mathbf{2}^{+}/\mathbf{2}^{2+}$ (Table 2) obtained with different supporting electrolytes for the same redox-active compound **2** under the same experimental conditions (solvent, concentration, scan rate, temperature) show that assignment of the nature of mixed-valent species based on the separation of formal electrode potentials of sequential redox processes is very dependent on the experimental setup and specifically very sensitive to the ion-pairing ability of the counterion employed, thereby shifting the equilibrium between the various oxidized species. In the present case with $[NBu_4][PF_6]$ as supporting electrolyte K_{com} equals 1.1×10^3, assigning the mixed-valent monocation $\mathbf{2}^{+}$ to the slightly delocalized Robin−Day[42] class II, whereas with $[NBu_4][B(C_6F_5)_4]$ as supporting electrolyte we obtain $K_{com} = 1.7 \times 10^5$ (Table 2), indicating $\mathbf{2}^{+}$ to be a "more delocalized" class II species.

2.2.2. [3]Cumulene. Figures 13 and 14 show the cyclic voltammetric profiles of [3]cumulene **11a** (an enriched sample of the trans isomer **11a** with only

(38) Fan, F.-R. F.; Yang, J.; Cai, L.; Price, D. W.; Dirk, S. M.; Kosynkin, D.; Yao, Y.; Rawlett, A. M.; Tour, J. M.; Bard, A. J. *J. Am. Chem. Soc.* **2002**, *124*, 5550.

(39) Creutz, C. *Progr. Inorg. Chem.* **1983**, *30*, 1, and references therein.

(40) (a) Launay, J.-P. *Chem. Soc. Rev.* **2001**, *30*, 386. (b) Launay, J.-P.; Coudret, C. In *Wires Based on Metal Complexes* in *Electron Transfer in Chemistry Vol. 5*; De Silva, A. P., Balzani, V., Eds.; Wiley-VCH: Weinheim, 2001; Chapter 1. (c) McCleverty, J. A.; Ward, M. D. *Acc. Chem. Res.* **1998**, *31*, 842. (d) Astruc, D. *Acc. Chem. Res.* **1997**, *30*, 383.

(41) (a) Camire, N.; Mueller-Westerhoff, U. T.; Geiger, W. E. *J. Organomet. Chem.* **2001**, *637−639*, 823. (b) LeSuer, R. J.; Geiger, W. *Angew. Chem., Int. Ed.* **2000**, *39*, 248.

(42) Robin, M. B.; Day, P. *Adv. Inorg. Chem. Radiochem.* **1967**, *10*, 247.

Table 2. Formal Electrode Potentials (V vs SCE), Peak-to-Peak Separations (mV), and K_{com} Values for the Redox Processes of 2, 11a, 22a,b, 4a,b, 17a,b,c, and 12a,b in Dichloromethane Solution

	oxidations						reductions			electrolyte
	$E^{\circ\prime}_{first}$	ΔE_p[a]	$E^{\circ\prime}_{2nd}$	ΔE_p[a]	K_{com}	E_{p3rd}[a]	$E^{\circ\prime}_{first}$	ΔE_p[a]	E_{p2nd}[a]	[Bu_4N][X]
2	+0.35	73	+0.53	95	1.1×10^3	+1.73				$E^{\circ\prime}_{second}$
	+0.33	95	+0.64	98	1.7×10^5					$B(C_6F_5)_4$
11a	+0.41	78	+0.60	80	1.6×10^3	+1.45	−1.20[b]		−1.6	PF_6
	+0.36	105	+0.74	112	2.6×10^6		−1.70	95	−2.15	$B(C_6F_5)_4$
22a,**b**	+0.42	80	+0.42	80	4	+1.40	−1.25[b]		−1.6	PF_6
	+0.39	90	+0.50	90	72	+1.65	−1.35	94	−1.72	$B(C_6F_5)_4$
4a,**b**	+0.56	140	+0.77	150	3.5×10^3	+1.45	−0.07[b]		−1.8	PF_6
	+0.56	110	+0.77	140	3.5×10^3	+1.45	−0.07[b]		−1.8	$B(C_6F_5)_4$
17a,**b**,**c**	+0.49	70	+0.61	72	1×10^2	+1.40	−0.04[b]		−1.2	PF_6
	+0.49	70	+0.61	90	1×10^2	+1.40	−0.04[b]		−1.4	$B(C_6F_5)_4$
12a,**b**	+0.42	90	+0.42	90	4	+1.50	−1.63	70	−2.0	PF_6
	+0.40	200	+0.54	150	2.3×10^2		−1.90[b]			$B(C_6F_5)_4$
FcH	+0.39	80								PF_6
	+0.42	180								$B(C_6F_5)_4$

[a] Measured at 0.1 V s^{-1}. [b] Peak potential values for irreversible processes.

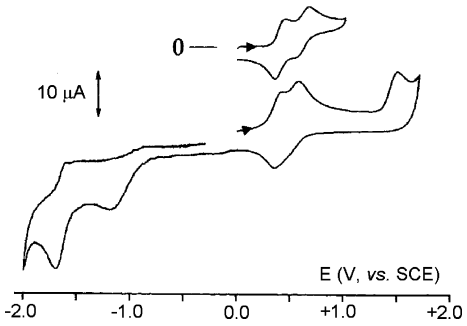

Figure 13. Cyclic voltammograms recorded at a platinum electrode in a CH_2Cl_2 solution containing **11a** (0.6×10^{-3} mol/L) and [NBu_4][PF_6] (0.2 mol/L). Scan rate 0.2 V s^{-1}.

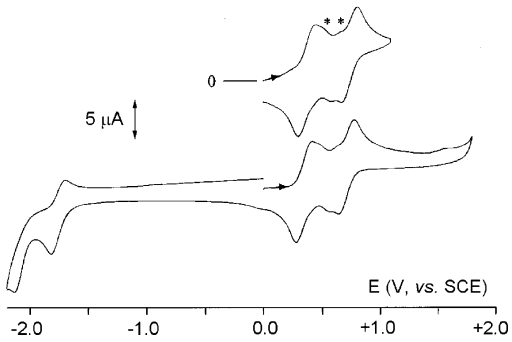

Figure 14. Cyclic voltammograms recorded at a platinum electrode in a CH_2Cl_2 solution containing **11a** (0.6×10^{-3} mol/L) and [NBu_4][$B(C_6F_5)_4$] (0.1 mol/L). Scan rate 0.2 V s^{-1}.

traces of cis isomer **11b**) with [NBu_4][PF_6] and [NBu_4][$B(C_6F_5)_4$] as the supporting electrolyte, respectively. In comparison to olefin **2**, the longer C_4-cumulene bridge between the redox termini affects only slightly the half-wave potentials of the ferrocenes (Table 2). The most significant difference is the appearance of multiple cumulene-centered reductions. Step-by-step controlled potential coulometry in correspondence to the ferrocene-centered oxidations proves that each one-electron process is chemically reversible. Upon the first one-electron removal ($E_w = +0.5$ V), the original dark red solution ($\lambda_{max(1)} = 560$ nm, $\lambda_{max(2)} = 420$ nm) turns brown, corresponding to a NIR charge transfer band at $\lambda_{max} = 920$ nm for the mixed-valent species **11a**$^+$. Further oxidation ($E_w = +1.0$ V) results in a brown-green solution ($\lambda_{max} = 630$ nm) after the overall consumption of 1.6 electrons per molecule.

With [NBu_4][$B(C_6F_5)_4$] as supporting electrolyte (Figure 14) the separation of the two ferrocene oxidations increases (Table 2) and the improved resolution[41] with the less-coordinating counteranion $[B(C_6F_5)_4]^-$ allows detection of additional minor processes (starred peaks in Figure 14), which we assign to traces of the cis isomer **11b** present in the sample of trans-enriched **11a**,**b**. On the basis of the separation of the two ferrocene redox couples **11a**/**11a**$^+$ and **11a**$^+$/**11a**$^{2+}$ the mixed-valent monocation **11a**$^+$ belongs to the slightly delocalized Robin−Day class II in the presence of [NBu_4][PF_6], but to the fully delocalized class III in the presence of [NBu_4]-[$B(C_6F_5)_4$] (Table 2).

2.2.3. [5]Cumulene. The cyclic voltammograms of [5]cumulene **22a**,**b** are shown in Figures 15 and 16 with the supporting electrolytes [NBu_4][PF_6] and [NBu_4]-[$B(C_6F_5)_4$], respectively. With hexafluorophosphate as counterion, a single ferrocene-based two-electron process occurs together with an irreversible oxidation and two irreversible reductions centered on the C_6 cumulene bridge (Figure 15, Table 2). In agreement with an i_{pc}/i_{pa} ratio lower than unity even at a scan rate of 1 V s^{-1} (for instance at 0.1 V s^{-1} the current ratio is equal to 0.7) for the ferrocene-centered process, controlled potential coulometry ($E_w = +0.8$ V) proves that the electrogenerated dication **22a**,**b**$^{2+}$ tends to decompose. Such a voltammetric profile obviously suggests that no interaction exists between the two ferrocenyl termini, corresponding to Robin−Day class I behavior. Nevertheless, with tetrakis(pentafluorphenyl)borate as counterion (Figure 16) two slighly separated redox waves are observed, which are more clearly visible in the Osteryoung square wave (OSW) voltammetry. The corresponding relative K_{com} value of 70 assigns monocation **22a**,**b**$^+$ to the slightly localized Robin−Day class II. In addition, the first cumulene reduction becomes chemically reversible.

2.2.4. Cumulenium Salts. A more complex redox pattern is observed in the case of the [2]cumulenium salt **4a**,**b** (Figure 17, Table 2). Both the cyclic and the Osteryoung voltammetric profiles suggest two slightly separated oxidation processes for the two ferrocenyl termini of this allenylium salt. Nevertheless, hydrodynamic voltammetry at an electrode with periodical

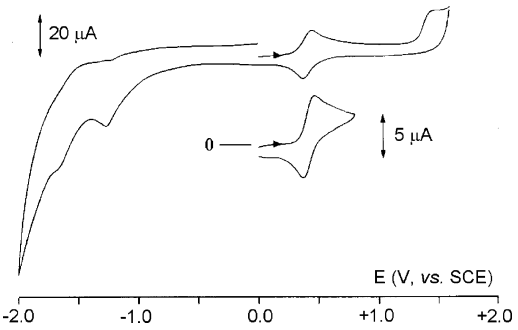

Figure 15. Cyclic voltammograms recorded at a platinum electrode in a CH_2Cl_2 solution containing **22a**,**b** (0.5×10^{-3} mol/L) and $[NBu_4][PF_6]$ (0.2 mol/L). Scan rates: top 0.2 V s^{-1}; bottom 0.1 V s^{-1}.

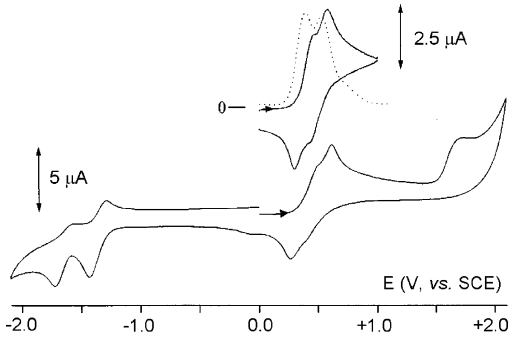

Figure 16. Cyclic (—) and Osteryoung square wave (···) voltammograms recorded at a platinum electrode in a CH_2Cl_2 solution containing **22a**,**b** (0.4×10^{-3} mol/L) and $[NBu_4][B(C_6F_5)_4]$ (0.1 mol/L). Scan rates: top 0.1 V s^{-1}; bottom 0.2 V s^{-1}.

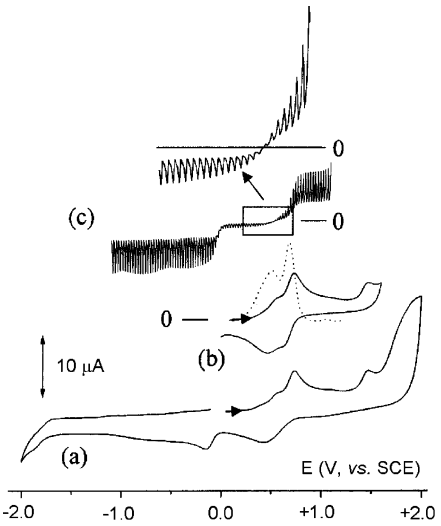

Figure 17. Cyclic (—), Osteryoung square wave (···), and hydrodynamic voltammograms recorded at a platinum electrode in a CH_2Cl_2 solution containing **4a**,**b** (0.7×10^{-3} mol/L) and $[NBu_4][PF_6]$ (0.2 mol/L). Scan rates: (a, b) 0.2 V s^{-1}; (c) 0.02 V s^{-1}.

renewal of the diffusion layer (see Experimental Section in the Supporting Information) reveals that the ferrocene subunit responsible for the first oxidation process is mostly oxidized, indicating that the positive charge of **4a**,**b** is delocalized not only through the three-carbon bridging group but also involving the charge-stabilizing ferrocenes. Exhaustive oxidation in correspondence to the most anodic ferrocene oxidation (E_w = +1.0 V)

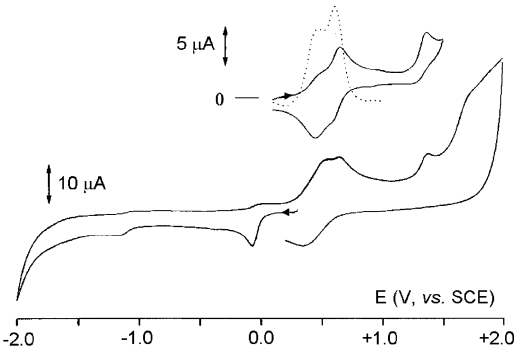

Figure 18. Cyclic (—) and Osteryoung square wave (···) voltammograms recorded at a platinum electrode in a CH_2Cl_2 solution containing **17a**,**b**,**c** (0.8×10^{-3} mol/L) and $[NBu_4][PF_6]$ (0.2 mol/L). Scan rate: 0.2 V s^{-1}.

consumes slightly more than one electron per molecule; the resulting solution exhibits a voltammetric response complementary to the original one, suggesting chemical reversibility. The cathodic step at −0.2 V corresponds to the reduction of the allenic/propargylic carbocation, in analogy to the reduction of other systems[43] like triphenylmethylium $[C(C_6H_5)_3]^+$ and tropylium $[C_7H_7]^+$. The separation between the ferrocene redox processes affords a K_{com} value of 3.5×10^3 for the mixed-valent species **4a**,**b**$^+$, which belongs therefore to the slightly delocalized Robin−Day class II. Unexpectedly, in this case no improvement in resolution was observed when $[NBu_4][B(C_6F_5)_4]$ was used instead of $[NBu_4][PF_6]$ as the supporting electrolyte.

The electrochemical properties of [4]cumulenium salt **17a**,**b**,**c** (Figure 18) are essentially similar to those of **4a**,**b**. Also in this case hydrodynamic voltammetry proves that the first ferrocene-centered process is constituted by a catho-anodic system. The original violet solution displays an intense and broad charge transfer band at λ_{max} = 940 nm. Exhaustive oxidation in correspondence to the second ferrocene-based process (E_w = +1.0 V) consumes 1.2 electrons per molecule and affords a brown solution, which gave a voltammetric profile quite complementary to the original one and which exhibited no charge transfer band at 940 nm. Also in this case the reduction process at about −0.05 V is assigned to the carbocation reduction, and similarly to the case of **4a**,**b** employment of $[NBu_4][B(C_6F_5)_4]$ did not improve the resolution of the redox waves.

2.2.5. Butadiene versus C_4-Cumulene. To compare the electrochemical properties of these cumulated compounds with a non-cumulene analogue, the cyclic voltammogram of butadiene **12a**,**b** was also recorded. Figure 19 ($[NBu_4][PF_6]$ as supporting electrolyte) and Figure 20 ($[NBu_4][B(C_6F_5)_4]$ as electrolyte) show that with hexafluorophosphate as counterion the first anodic process involves simultaneous oxidation of the two ferrocenyl ligands by a two-electron process, whereas with tetrakis(pentafluorophenyl)borate as counterion a slight separation of two one-electron processes is visible, corresponding to a relative comproportionation constant ($K_{com} = 2 \times 10^2$) of the monocation **12a**,**b**$^+$ at the lowest limits of a slightly localized mixed-valent compound (Table 2). Because **12a**,**b** is a mixture of diasteroisomers (vide supra), the CVs show additional shoulders (starred

(43) Connelly, N. G.; Geiger, W. E. *Chem. Rev.* **1996**, *96*, 877.

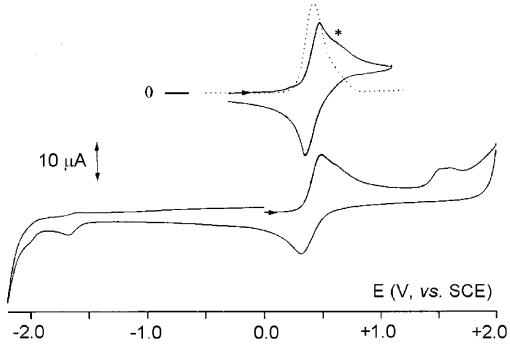

Figure 19. Cyclic (—) and Osteryoung square wave (···) voltammograms recorded at a platinum electrode in a CH_2Cl_2 solution containing **12a**,**b** (0.9×10^{-3} mol/L) and $[NBu_4][PF_6]$ (0.2 mol/L). Scan rate: 0.2 V s^{-1}.

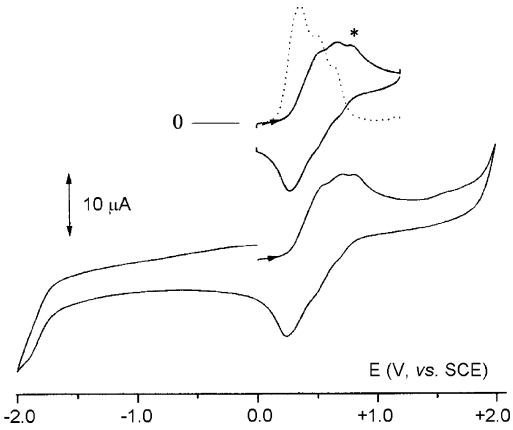

Figure 20. Cyclic (—) and Osteryoung square wave (···) voltammograms recorded at a platinum electrode in a CH_2Cl_2 solution containing **12a**,**b** (0.6×10^{-3} mol/L) and $[NBu_4][B(C_6F_5)_4]$ (0.1 mol/L). Scan rate: 0.2 V s^{-1}.

peaks) which are attributed to isomeric butadiene species. Most significant is the result that a butadiene moiety C═CH−CH═C is *less* conjugated than a C_4 cumulene C═C═C═C, as evidenced by the larger separation of the first and second oxidation in the latter case (compare Table 2).

2.2.6. Summary of Cumulene Electrochemistry. In summary we can conclude (Table 2) that (i) cumulenic compounds with two terminal ferrocenyl groups have a first oxidation potential roughly similar to that of unsubstituted ferrocene (with the exception of the cationic systems **4a**,**b** and **17a**,**b**,**c**). (ii) The separation of the first and second redox process decreases with increasing length of the cumulene, as anticipated. Olefin **2** exhibits less separation in comparison to [3]cumulene **11a**, due to the steric strain in this olefin, which has noncoplanar phenyl substituents (vide supra) that reduce the electron density of the π-system. (iii) By electrochemical methods the electronic communication between the terminal ferrocenyl groups can be detected up to a chain length of six carbons, corresponding to a 6.5 Å (length of the cumulene bridge) or 11.4 Å (distance between Fe redox sites) molecular wire, respectively. (iv) The best compromise between chemical stability and charge transport along a cumulene system shows the [3]cumulene system, suggesting butatriene C═C═C═C building blocks as attractive components of future conducting molecular rigid rods. (v) In comparison to oligo-olefinic compounds, cumulenes show a better performance as molecular wires, at least for the short systems here under study.

3. Experimental Section

General Procedures. Reactions were conducted in Schlenk tubes under Ar atmospheres by techniques common in organometallic chemistry. Commercially available starting materials were used as received. Solvents were dried, deoxygenated, and saturated with Ar. Standard instrumentation and techniques for spectroscopic and physical measurements (NMR, Raman, IR, MS, etc.) have been described previously.[44] Crystallographic and electrochemical procedures are detailed in the Supporting Information acompanying this paper.

1,2-Diferrocenyl-1,2-diphenylethene (2). A Schlenk tube was charged with 2.1 g (3.52 mmol) of $TiCl_3 \cdot AlCl_3$, 150 mL of dimethoxyethene, and 0.29 g (41.8 mmol) of Li powder. The pale blue mixture was sonicated in an ultrasonic cleaning bath for half an hour; during this process the mixture became black, indicating formation of reduced Ti species. After addition of 1 g (3.45 mmol) of benzoyl ferrocene (**1**), the mixture was sonicated under Ar atmosphere for an additional hour. Work-up: Without protection from air, the mixture was hydrolyzed with ice/water and washed with four portions of diethyl ether, the combined organic layers were dried with Na_2SO_4, and the organic solvents were removed on a rotary evaporator, yielding the crude product mixture consisting of **2** and the over-reduced byproduct diferrocenyldiphenylethane. Column chromatography on basic alumina with *n*-hexane/ether (v/v = 5:3) afforded 0.22 g of **2** in 23.1% yield: orange crystals, mp 272−277 °C. Anal. Calcd for $C_{34}H_{28}Fe_2$: C, 74.48; H, 5.15. Found: C, 74.51; H, 5.10. IR (KBr): 3087 w, 2963, m, 2929 m, 2857 m, 1728 m, 1638 m, 1599 m, 1491 w, 1452 w, 1441 m, 1412 m, 1385 w, 1261 s, 1105 s, 1076 m, 1026 s, 999 m, 928 m, 891 w, 812 s, 769 w, 721 m, 708 m, 698 m, 492 s cm^{-1}. Raman: 1597 w, 1572 s ($\nu_{C=C}$), 1432 w cm^{-1}. UV−vis (CH_2Cl_2; λ_{max}/ϵ): 240.0/19800, 321.5/14200, 468/1520 nm (Figure 8). MS (FAB): 549 ($M^+ + H$, 46%), 548 (M^+, 100%) *m/e*. ^1H NMR data concur with published values.[14] ^{13}C NMR (CD_2Cl_2): 143.4 (C═C); 135.1, 130.5, 128.8, 127.2 (phenyl); 87.5, 69.8, 69.5, 68.8 (Cp) ppm. Single crystals were obtained from a dichloromethane solution (Figure 1).

1,3-Diferrocenyl-1-phenylpropynol (3). A Schlenk vessel was charged with 0.5 g (2.38 mmol) of ferrocenylethyne[15] and 100 mL of THF. A 1.2 mL sample of a 2 M *n*-hexane solution of *n*-butyllithium (2.4 mmol) was added at a temperature of −60 °C. The stirred mixture was allowed to warm to room temperature, and 0.5 g (1.72 mmmol) of **1** was added in one portion under protection from air. After stirring overnight, 5 mL of water was added, volatile materials were removed on a rotary evaporator, the yellow solid residue was dissolved in dichloromethane, the organic phase was washed twice with a 5% aqueous $NaHCO_3$ solution and once with water, the organic layer was separated and dried with Na_2SO_4, and dichloromethane was removed on a rotary evaporator, yielding the crude yellow product. Column chromatography on basic alumina with a *n*-hexane/ether (v/v = 1:1) mixture as eluent afforded 0.58 g of **3** in 68.5% yield: yellow powder, mp 110−115 °C. Anal. Calcd for $C_{29}H_{24}Fe_2O$: C, 69.64; H, 4.48. Found: C, 69.58; H, 4.52. IR (KBr): 3544 m (ν_{OH}), 3089 w, 2222 m ($\nu_{C\equiv C}$), 1640 w, 1601 w, 1498 m, 1449 m, 1412 m, 1389 w, 1323 m, 1310 m, 1221 w, 1165 m, 1105 m, 1065 w, 1043 m, 1030 m, 1018 m, 1001 m, 928 m, 904 w, 821 s, 764 s, 702 s, 684 w, 673 w, 528 w, 515 w, 486 s, 424 w cm^{-1}. MS (EI): 500 (M^+, 28%), 362 (M^+ − Cp, Fe, OH; 40%), 291 (FcPhCOH, 21%), 290 (FcPhCO, 100%), 210 (Fc-C≡CH, 73%) *m/e*. ^1H NMR ($CDCl_3$): 7.65 (2H, d, phenyl); 7.32 (3H, m, phenyl); 4.52 (2H, m, Cp);

(44) Bildstein, B.; Malaun, M.; Kopacka, H.; Wurst, K.; Mitterböck, M.; Ongania, K.-H.; Opromolla, G.; Zanello, P. *Organometallics* **1999**, *18*, 4325.

4.46 (1H, m, Cp); 4.38 (1H, m, Cp); 4.36 (s, 5H, Cp); 4.27 (5H, s, Cp); 4.25 (3H, m, Cp); 4.18 (1H, m, Cp); 3.12 (1H, s, OH) ppm. ^{13}C NMR ($CDCl_3$): 144.3, 128.0, 127.5, 125.5 (phenyl); 97.3, 88.5, 83.7 (propyne); 71.9, 71.4, 69.9, 68.8, 68.4, 68.3, 68.2, 65.1, 64.7 (Cp) ppm. Single crystals were obtained from a dichloromethane/ether solution (Figure 2).

1,3-Diferrocenyl-1-phenylallenylium Tetrafluoroborate (4a,b). A Schlenk tube was charged with 0.5 g (0.10 mmol) of **3** and 50 mL of diethyl ether, giving a yellow solution. Under protection from air, 16 mL of a 54% ethereal HBF_4 solution (0.12 mmol) was added. Immediatly a dark green precipitate of the product was formed. After the suspension was stirred for 10 min, the precipitate was filtered off, washed with diethyl ether, and dried by oil pump vacuum, affording 45 mg of **4a**,**b** in 78.2% yield: green powder, mp not observed, decomposition > 320 °C. Anal. Calcd for $C_{29}H_{23}BF_4Fe_2$: C, 61.11; H, 4.07. Found: C, 60.88; H, 4.02. IR (KBr): 3105 w, 2137 s ($\nu_{C=C=C+}$), 1636 m, 1591 w, 1491 w, 1451 m, 1414 w, 1385 m, 1342 m, 1329 m, 1234 w, 1182 m, 1124 m, 1107 m, 1084 s, 1045 m, 1036 m, 1018 m, 837 m, 825 m, 727 w, 700 w, 669 w, 615 w, 588 w, 534 w, 493 m, 476 m, 439 w cm^{-1}. UV−vis (CH_2Cl_2; λ_{max}/ϵ): 397.0/3614, 446.0/3489, 868.7/7650 nm (Figure 9). MS (FAB): 484 (M^+ + H, 43%), 483 (M^+, 100%) *m/e*. ^{1}H NMR (CD_2Cl_2): 7.86 (3H, m, phenyl); 7.49 (2H, t, phenyl); 6.42, 5.51, 4.98, 4.89 (each signal: 2H, m, Cp); 4.72, 4.40 (both signals: 5H, s, Cp) ppm. ^{13}C NMR (CD_2Cl_2): 143.9 (allenylium); 138.6, 133.6, 130.6, 129.6 (phenyl); 127.5, 101.4 (allenylium); 100.7, 91.6, 82.4, 75.9, 74.7, 72.9, 63.4 (Cp) ppm.

1,3,4,6-Tetraferrocenyl-1,4-diphenylhexa-1,2-dien-5-yne (6). A Schlenk tube was charged with 0.228 g (0.40 mmol) of **4a**,**b** and 150 mL of benzene. The mixture was cooled to 10 °C, and 0.25 mL of a 1.8 M cyclohexane/ether solution of phenyllithium (0.45 mmol) was added. An immediate color change from green to orange occurred. The mixture was sonicated in an ultrasound cleaning bath for 1 h and stirred at room temperature for an additional hour. Workup: insoluble materials were removed by filtration through a short plug of alumina, solvents were removed on a rotary evaporator, and the residue was chromatographed on basic alumina with a mixture of *n*-hexane/ether (v/v = 2:1) as eluent, affording 60 mg of **6** in 27.8% yield: yellow powder, mp 191 °C (dec). Anal. Calcd for $C_{58}H_{46}Fe_4$: C, 72.09; H, 4.80. Found: C, 72.13; H, 4.77. IR (KBr): 2957 m, 2919 s, 2849 s, 1636 m, 1462 m, 1412 w, 1385 m, 1261 m, 816 s, 766 w, 729 m, 700 m, 484 m cm^{-1}. MS (FAB): 967 (M^+ + H, 6%), 966 (M^+, 6%), 559 (FcPhC=C=CFcCCp, 5%), 485 (FcPhC=C=CFc + 2H, 7%), 484 (FcPhC=C=CFc + H, 35%), 483 (FcPhC=C=CFc, 100%) *m/e*. ^{1}H NMR (CD_2Cl_2): 7.93 (2H, d, phenyl); 7.85 (2H, d, phenyl); 7.78 (2H, d, phenyl); 7.56 (2H, d, phenyl); 7.44 (6H, m, phenyl); 7.38 (6H, m, phenyl); 4.60 (1H, m, Cp); 4.59 (2H, m, Cp); 4.56 (2H, m, Cp); 4.53 (1H, m, Cp); 4.44 (1H, m, Cp); 4.35 (2H, m, Cp); 4.32 (5H, s, Cp); 4.30 (5H, s, Cp); 4.28 (4H, m, Cp); 4.275 (1H, m, Cp); 4.27 (1H, m, Cp); 4.26 (1H, m, Cp); 4.25 (2H, m, Cp); 4.23 (5H, s, Cp); 4.22 (1H, m, Cp); 4.20 (5H, s, Cp); 4.18 (1H, m, Cp); 4.08 (2H, m, Cp); 4.06 (2H, m, Cp); 4.02 (1H, m, Cp); 4.00 (5H, s, Cp); 3.99 (1H, m, Cp); 3.98 (5H, s, Cp); 3.96 (1H, m, Cp); 3.95 (2H, m, Cp); 3.92 (1H, m, Cp); 3.91 (5H, s, Cp); 3.88 (5H, s, Cp); 3.70 (1H, m, Cp); 3.60 (1H, m, Cp) ppm. ^{13}C NMR (CD_2Cl_2): 206.3, 205.9 (C=C=C); 142.8, 142,4, 137.6, 137.2, 128.9, 128.8, 128.6, 128.5, 128.4, 128.35, 127.9, 127.8, 127.5, 127.4, 127.35, 127.3 (phenyl); 115.5, 115.4, 110.9, 119.6 (C=C=C); 95.7, 95.6, 89.4, 89.38 (C≡C); 84.8, 84.6 (propyne); 83.4, 83.1, 82.6, 82.5, 71.8, 71.7, 70.1, 70.08, 69.8, 69.7, 69.67, 69.6, 69.3, 69.1, 69.03, 68,96, 68.8, 68.7, 68.68, 67.9, 67.8, 67.7, 67.67, 67.6, 67.5, 67.47, 66.6 (Cp) ppm.

1-Ferrocenyl-3-trimethylsilyl-1-phenylpropynol (7). A Schlenk vessel was charged with 150 mL of THF and 1.7 mL (12.03 mmol) of trimethylsilylethyne. After cooling of the solution to −60 °C, 6.1 mL of a 2 M *n*-butyllithium solution (12.20 mmol) was added, and the stirred mixture was allowed to warm to room temperature. A 2.5 g (8.62 mmol) sample of **1** was added in one portion under protection from air, and the mixture was stirred at room temperature over the weekend (ca. 60 h). Workup: 5 mL of water was added, solvents were removed on a rotary evaporator, the crude yellow residue was dissolved in dichloromethane, the organic solution was washed with two portions of aqueous $NaHCO_3$ and with one portion of water, the dichloromethane solution was dried with Na_2SO_4, the solvent was removed on a rotary evaporator, and the residue was chromatographed on basic alumina with *n*-hexane/ether (v/v = 2:1) as eleuent, affording 2.3 g of **7** in 68.6% yield, together with the desilylated side product 1-ferrocenyl-1-phenylpropynol in 22.0% yield.

Data for **7**: yellow powder, mp 127−130 °C. Anal. Calcd for $C_{22}H_{24}FeOSi$: C, 68.04; H, 6.23. Found: C, 68.00; H, 6.22. IR (KBr): 3534 m (ν_{OH}), 2963 w, 2902 w, 2178 w ($\nu_{C\equiv C}$), 1634 w, 1599 w, 1489 m, 1447 m, 1412 w, 1389 w, 1333 m, 1304 w, 1259 s, 1248 m (n_{Si-C}), 1232 w, 1159 m, 1107 m, 1088 m, 1072 w, 1053 s, 1043 m, 1032 m, 1021 m, 999 m, 924 m, 849 s, 832 m, 816 m, 807 m, 766 m, 708 m, 694 m, 642 w, 605 w, 521 m, 490 s, 452 w, 426 m cm^{-1}. MS (FAB): 391 (M^+ + 3H, 2%), 390 (M^+ + 2H, 12%), 389 (M^+ + H, 52%), 388 (M^+, 100%), 387 (M^+ − H, 5%) *m/e*. ^{1}H NMR ($CDCl_3$): 7.61 (2H, d, phenyl); 7.31 (3H, m, phenyl); 4.40 (1H, m, Cp); 4.36 (1H, m, Cp); 4.31 (5H, s, Cp); 4.22 (1H, m, Cp); 4.16 (1H, m, Cp); 3.10 (1H, s, OH); 0.32 (9H, s, $Si(CH_3)_3$) ppm. ^{13}C NMR ($CDCl_3$): 143.7, 127.9, 127.5, 125.5 (phenyl); 108.2, 96.7, 89.2 (propyne); 71.6, 68.9, 68.4, 68.2, 64.9 (Cp); 0.0 ($Si(CH_3)_3$) ppm.

Data for 1-ferrocenyl-1-phenylpropynol: yellow powder, mp 85−89 °C. IR (KBr): 3546 m (ν_{OH}), 3287 s ($\nu_{C\equiv C-H}$), 3085 w, 3058 w, 3027 w, 2114 w ($\nu_{C\equiv C}$), 1759 w, 1636 m, 1599 m, 1489 s, 1449 s, 1412 m, 1389 m, 1377 m, 1329 s, 1304 m, 1285 m, 1261 m, 1234 m, 1182 w, 1157 s, 1105 s, 1051 s, 1043 m, 1022 m, 1001 s, 991 m, 918 s, 864 w, 843 m, 823 s, 816 s, 758 s, 702 s, 688 s, 663 s, 586 m, 524 m, 515 m, 486 s, 451 m, 439 m, 405 w cm^{-1}. MS (FAB): 318 (M^+ + 2H, 4%), 317 (M^+ + H, 22%), 316 (M^+, 100%), 315 (M^+ − H, 3%) *m/e*. ^{1}H NMR ($CDCl_3$): 7.59 (2H, d, phenyl); 7.31 (3H, m, phenyl); 4.47 (1H, m, Cp); 4.31 (5H, s, Cp); 4.30 (1H, m, Cp); 4.25 (1H, m, Cp); 4.17 (1H, m, Cp); 3.20 (1H, s, OH); 2.80 (1H, s, C≡C−H) ppm. ^{13}C NMR ($CDCl_3$): 143.6, 128.0, 127.6, 125.4 (phenyl); 96.5, 86.7, 73.0 (propyne); 71.0, 68.9, 68.4, 68.2, 65.0 (Cp) ppm.

1-Ferrocenyl-1-methoxy-3-trimethylsilyl-1-phenylpropyne (8). A Schlenk vessel was charged with 2.8 g (7.21 mmol) of **7** and 150 mL of THF. The solution was cooled to −60 °C, and 5.0 mL of a 1.6 M ethereal methyllithium solution (8.00 mmol) was added. The stirred solution was allowed to warm to −25 °C, then 0.9 mL (14.47 mmol) of iodomethane was added and stirring was continued overnight at room temperature. Workup: solvents and volatile materials were removed on a rotary evaporator, the oily residue was dissolved in ether, and the organic solution was washed with $NaHCO_3$ and H_2O and dried with Na_2SO_4. After removal of ether, 2.45 g of **8** was obtained in 84.3% yield: yellow powder, mp 140−143 °C. Anal. Calcd for $C_{23}H_{26}FeOSi$: C, 68.65; H, 6.51. Found: C, 68.61; H, 6.48. IR (KBr): 3000 w, 2948 w, 2934 w, 2902 w, 2824 w, 2163 w ($\nu_{C\equiv C}$), 1636 m, 1489 w, 1449 m, 1435 w, 1414 w, 1387 w, 1250 s (ν_{Si-C}), 1217 w, 1192 m, 1177 m, 1157 w, 1105 m, 1080 s, 1057 s, 1036 m, 1020 m, 1005 m, 941 m, 860 s, 827 s, 812 s, 766 s, 719 m, 700 s, 638 m, 603 w, 582 m, 520 m, 505 m, 495 m, 484 m, 465 w cm^{-1}. MS (FAB): 403 (M^+ + H, 34%), 402 (M^+, 100%), 371 (M^+ − OCH_3, 30%), 298 (M^+ − $Si(CH_3)_3$) *m/e*. ^{1}H NMR ($CDCl_3$): 7.13 (2H, d, phenyl); 7.39 (3H, m, phenyl); 4.53 (1H, m, Cp); 4.18 (1H, m, Cp); 4.16 (5H, s, Cp); 4.08 (1H, m, Cp); 3.97 (1H, m, Cp); 3.33 (3H, s, OCH_3); 0.39 (9H, s, $Si(CH_3)_3$) ppm. ^{13}C NMR ($CDCl_3$): 141.3, 127.8, 127.7, 126.8 (phenyl); 104.3, 93.6, 92.7 (propyne); 79.3, 69.3, 67.8, 67.3, 66.8 (Cp); 52.6 (OCH_3); 0.09 ($Si(CH_3)_3$) ppm.

1-Ferrocenyl-1-methoxy-1-phenylpropyne (9). A Schlenk tube was charged with 2.45 g (43.7 mmol) of solid KOH, 100 mL of dry methanol, and 1.76 g (4.37 mmol) of **8**. The suspension was stirred for 12 h at ambient temperature.

Workup: solvents and volatile materials were removed on a rotary evaporator, the solid residue was dissolved in ether, the organic solution was washed with two portions of an aqueous 5% $NaHCO_3$ solution and once with water, and the organic phase was dried with Na_2SO_4 and evaporated, affording 1.26 g of **9** in 84.2% yield: yellow powder, mp 75−78 °C. Anal. Calcd for $C_{20}H_{18}FeO$: C, 72.75; H, 5.49. Found: C, 72.82; H, 5.52. IR (KBr): 3247 s ($\nu_{C\equiv C-H}$), 3087 w, 2981 w, 2957 w, 2932 w, 2898 w, 2822 w, 2118 w ($\nu_{C\equiv C}$), 1636 m, 1491 w, 1464 m, 1451 w, 1408 m, 1395 w, 1319 w, 1252 m, 1227 m, 1192 m, 1178 m, 1105 m, 1065 s, 1057 m, 1043 s, 1020 s, 999 m, 980 w, 953 w, 933 m, 918 m, 870 w, 860 w, 848 m, 816 s, 725 s, 708 s, 688 s, 669 m, 594 m, 522 m, 503 m, 484 m, 465 m, 447 w cm^{-1}. MS (FAB): 331 ($M^+ + H$, 24%), 330 (M^+, 100%), 299 ($M^+ - H$, 24%) *m/e*. ^1H NMR ($CDCl_3$): 7.70 (2H, d, phenyl); 7.38 (3H, m, phenyl); 4.47 (1H, m, Cp); 4.17 (1H, m, Cp); 4.14 (5H, s, Cp); 4.09 (1H, m, Cp); 4.00 (1H, m, Cp); 3.32 (3H, s, OCH_3); 2.94 (1H, s, C≡C−H) ppm. ^{13}C NMR ($CDCl_3$): 141.1, 127.8, 127.78, 126.7 (phenyl); 93.6, 82.7, 79.0 (propyne); 76.1, 69.3, 67.9, 67.87, 67.2, 66.8 (Cp); 52.7 (OCH_3) ppm. Single crystals were obtained from layering a dichloromethane solution with ether (Figure 3).

1,4-Diferrocenyl-4-methoxy-1,4-diphenylbut-2-ynol (10). A Schlenk vessel was charged with 0.5 g (1.51 mmol) of **9** and 150 mL of THF, the solution was cooled to −60 °C, and 0.8 mL of a 2.0 M *n*-butyllithium solution (1.60 mmol) was added via syringe. The stirred mixture was allowed to warm to room temperature, and 0.44 g (1.52 mmol) of **1** was added in one portion with protection of the reaction mixture from air. After stirring for 18 h, the mixture was worked up: 5 mL of water was added, solvents were removed on a rotary evaporator, the residue was dissolved in ether, the organic solution was washed with three portions of water, the organic layer was dried with Na_2SO_4, ether was removed in vacuo, and the crude residue was chromatographed on basic alumina with *n*-hexane/ether (v/v = 2:1) as eluent, affording 0.68 g of **10** in 72.7% yield: orange powder, mp 171−172 °C. Anal. Calcd for $C_{37}H_{32}Fe_2O_2$: C, 71.64; H, 5.20. Found: C, 71.54; H, 5.17. IR (KBr): 2548 m (ν_{OH}), 3089 w, 2932 w, 2853 w, 2203 w ($\nu_{C\equiv C}$), 1634 m, 1601 m, 1586 m, 1491 s, 1449 s, 1412 m, 1391 m, 1321 m, 1263 m, 1234 m, 1182 m, 1165 m, 1138 m, 1105 s, 1092 s, 1076 s, 1051 m, 1030 m, 1007 s, 943 m, 908 m, 825 s, 756 m, 677 s, 648 m, 609 w, 584 w, 519 s, 499 s, 459 w, 409 w cm^{-1}. MS (FAB): 622 ($M^+ + 2H$, 10%), 621 ($M^+ + H$, 40%), 620 (M^+, 100%), 619 ($M^+ - H$, 6%), 618 ($M^+ - 2H$, 11%), 603 ($M^+ - OH$, 8%), 589 ($M^+ - OCH_3$, 12%) *m/e*. ^1H NMR ($CDCl_3$): 7.74 (2H, d, phenyl); 7.68 (2H, d, phenyl); 7.34 (6H, m, phenyl); 4.66 (1H, m, Cp); 4.38 (1H, m, Cp); 4.31 (5H, s, Cp); 4.30 (1H, m, Cp); 4.27 (1H, m, Cp); 4.21 (1H, m, Cp); 4.12 (1H, m, Cp); 4.05 (1H, m, Cp); 4.00 (1H, m, Cp); 3.96 (5H, s, Cp); 3.39 (3H, s, OCH_3); 3.31 (1H, s, OH) ppm. ^{13}C NMR ($CDCl_3$): 144.4, 141.6, 128.1, 127.9, 127.8, 127.6, 126.9, 125.5 (phenyl); 97.5, 93.8, 91.3, 84.2 (butyne); 79.3, 71.2, 69.2, 68.8, 68.2, 68.8, 67.9, 67.2, 67.1, 65.3 (Cp); 53.0 (OCH_3) ppm. Single crystals were obtained from a dichloromethane solution (Figure 4).

1,4-Diferrocenyl-1,4-diphenylbutatriene (11a,b). A round-bottom flask was charged with 0.1 g (0.16 mmol) of **10** and 50 mL of methanol. To this stirred suspension was added a solution of 32 mg (0.17 mmol) of $SnCl_2$ in 5 mL of aqueous 50% acetic acid, and the mixture was refluxed for 30 min. Workup: the mixture was cooled to room temperature and hydrolyzed by addition of water, organic materials were extracted into dichloromethane, the organic phase was washed with two portions of water, the organic solution was dried with Na_2SO_4, solvents were removed on a rotary evaporator, and the crude product mixture was chromatographed on basic alumina with *n*-hexane/ether (v/v = 5:1), affording 21 mg of *trans*-1,4-diferrocenyl-1,4-diphenylbutatriene (**11a**) and *cis*-1,4-diferrocenyl-1,4-diphenylbutatriene (**11b**) in 23% combined yield as an unseparable 1:1 cis/trans **11a**,**b** mixture: burgundy red powder, mp >199 °C (dec). Anal. Calcd for $C_{36}H_{28}Fe_2$: C, 75.55; H, 4.93. Found: C, 75.60; H, 4.94. IR (KBr): 2965 m, 2929 w, 2025 very w ($\nu_{C=C=C=C}$), 1636 m, 1489 m, 1441 m, 1412 m, 1385 m, 1288 w, 1261 s, 1105 s, 1088 s, 1047 s, 1024 s, 945 w, 820 s, 764 m, 712 m, 696 s, 667 w, 592 w, 495 s, 405 w cm^{-1}. Raman IR: 2024 s ($\nu_{C=C=C=C}$), 1587 w, 1487 w, 1452 w, 1376 w, 1333 w, 1282 w, 1236 w, 1194 w, 1178 w, 1102 w, 1055 w, 994 w, 828 w, 664 w cm^{-1}. UV−vis (CH_2Cl_2; λ_{max}/ϵ): 281.0/13674, 337.0/14200, 449.0/6802, 576.0/2279 nm (Figure 8). MS (FAB): 573 ($M^+ + H$, 31%), 572 (M^+, 54%), 451 ($M^+ -$ CpFe, 100%) *m/e*. ^1H NMR (CD_2Cl_2): 7.87 (4H, d, phenyl); 7.74 (4H, d, phenyl); 7.47 (6H, m, phenyl); 7.39 (6H, m, phenyl); 4.78 (4H, m, Cp); 4.61 (4H, m, Cp); 4.51 (4H, m, Cp); 4.42 (4H, m, Cp); 4.27 (10H, s, Cp); 4.19 (10H, s, Cp) ppm. ^{13}C NMR (CD_2Cl_2): 147.2, 147.1 (C=C=C=C); 139.8, 139.6, 128.9, 128.7, 128.6, 127.8, 127.7 (phenyl); 119.4, 119.3 (C=C=C=C); 84.8, 84.7, 70.5, 70.3, 70.2, 70.1, 69.53, 69.48 (Cp) ppm. Single crystals of isomer **11b** were obtained from a dichloromethane/ether solution (Figure 5).

1,4-Diferrocenyl-1,4-diphenylbuta-1,3-diene (12a,b). A Schlenk tube was charged with 0.32 g (0.54 mmol) of $TiCl_3 \cdot AlCl_3$, 40 mg (5.76 mmol) of Li powder, and 150 mL of dimethoxyethane, and the mixture was sonicated in an ultrasound cleaning bath for 30 min. The initially pale blue suspension became black during sonication, indicating formation of reduced Ti species. After addition of 0.2 g (0.32 mmol) of **10**, sonication was continued for 1 h. Workup: the mixture was poured onto ice/water, organic materials were extracted into ether, and the organic solution was dried with Na_2SO_4 and evaporated, affording 29 mg of **12a**,**b** in 15.3% yield as a 1:1 mixture of isomers: red powder, mp 165−168 °C. Anal. Calcd for $C_{36}H_{30}Fe_2$: C, 75.29; H, 5.26. Found: C, 75.43; H, 5.28. IR (KBr): 3258 m, 2963 m, 2927 w, 2855 w, 2071 w ($\nu_{C=C}$), 1715 m, 1634 s, 1553 w, 1489 m, 1454 m, 1261 s, 1107 s, 1026 s, 808 s, 764 m, 696 m, 594 w, 495 w, 480 m cm^{-1}. MS (FAB): 575 ($M^+ + H$, 44%), 574 (M^+, 100%), 572 ($M^+ - 2H$, 21%), 288 ($FcPhC{=}CH_2$, 18%), 275 (FcPhCH, 70%) *m/e*. ^1H NMR (CD_2Cl_2): 7.87 (4H, d, phenyl); 7.75 (4H, d, phenyl); 7.39 (16H, m, phenyl + C=CH); 4.79 (2H, m, Cp); 4.61 (4H, m, Cp); 4.51 (2H, m, Cp); 4.43 (4H, m, Cp); 4.27 (10H, s, Cp); 4.19 (10H, s, Cp); 4.14 (2H, m, Cp); 4.04 (2H, m, Cp) ppm. ^{13}C NMR (CD_2Cl_2): 147.17, 147.07 (C=C); 139.8, 139.6, 128.9, 128.7, 128.6, 128.5, 128.4, 127.8, 127.6 (phenyl); 119.37, 119.24 (C=C); 84.8, 84.7, 70.4, 70.3, 70.2, 70.1, 69.7, 69.5, 69.45, 69.0 (Cp) ppm.

1-Ferrocenyl-1-phenylbut-3-ynol (14). An ethereal allenyl/propargyl (**13a**,**b**) Grignard solution (10.4 mmol) was prepared according to literature procedures[25] and cooled to −40 °C. To this solution was added a suspension of 2.0 g (6.89 mmol) of **1** in 100 mL of ether during a period of 30 min. The stirred mixture was allowed to warm to room temperature and worked up: the mixture was hydrolyzed by pouring it on ice/water, 1.0 g of NH_4Cl was added, the organic/aqueous phases were separated, the aqueous layer was extracted two times with ether, the combined organic phases were washed with three portions of water, the solution was dried with Na_2SO_4, and solvents and volatile materials were removed in vacuo on a rotary evaporator, affording 1.9 g of **14** in 84.8% yield: orange powder, mp 118−120 °C. Anal. Calcd for $C_{20}H_{18}FeO$: C, 72.75; H, 5.49. Found: C, 72.68; H, 5.46. IR (KBr): 3558 s (ν_{OH}), 3289 s ($\nu_{C\equiv C-H}$), 3079 w, 2909 w, 2124 w ($\nu_{C\equiv C}$), 1636 m, 1601 w, 1489 m, 1445 m, 1410 m, 1385 m, 1354 w, 1341 m, 1261 m, 1236 w, 1200 m, 1161 m, 1105 s, 1095 m, 1065 s, 1053 m, 1028 m, 1013 s, 999 m, 974 w, 877 w, 839 m, 820 s, 766 m, 712 s, 694 m, 677 m, 656 s, 638 m, 548 m, 507 m, 497 w, 490 m, 474 m cm^{-1}. MS (FAB): 332 ($M^+ + 2H$, 3%), 331 ($M^+ + H$, 18%), 330 (M^+, 100%), 329 ($M^+ - H$, 3%), 328 ($M^+ - 2H$, 5%), 314 ($M^+ - OH + H$, 4%), 313 ($M^+ - OH$, 16%), 312 ($M^+ - OH - H$, 2%), 291 (FcPhCOH, 6%), 290 (FcPhCO, 2%), 274 (FcPhC, 1%), 248 ($M^+ - OH - Cp$, 1%), 247 ($M^+ - OH - Cp - H$, 5%), 192 ($M^+ - OH -$ CpFe, 1%), 191 ($CpPhCCH_2C{\equiv}C$, 3%), 186 (Fc + H, 8%), 105 (PhCO, 17%) *m/e*. ^1H NMR ($CDCl_3$): 7.43

(2H, d, phenyl); 7.32 (3H, m, phenyl); 4.43 (1H, m, Cp); 4.25 (1H, m, Cp); 4.23 (5H, s, Cp); 4.16 (1H, m, Cp); 4.05 (1H, m, Cp); 3.07 (2H, d, CH_2); 3.05 (1H, s, OH); 2.03 (1H, t, C≡C−H) ppm. ^{13}C NMR ($CDCl_3$): 144.9, 127.6, 126.8, 125.5 (phenyl); 98.5 (C°C); 80.5 (C(1) of butynol); 73.6 (C≡C); 71.5, 68.6, 68.2, 67.8, 66.9, 66.7 (Cp); 34.4 (CH_2 of butynol) ppm. Single crystals were obtained from a dichloromethane solution (Figure 6).

1-Ferrocenyl-1-methoxy-1-phenylbut-3-yne (15). A Schlenk flask was charged with 2.05 g (6.21 mmol) of **14** and 150 mL of THF and cooled to −70 °C. Under protection from air, 3.26 mL of a 2.0 M pentane solution of *n*-butyllithium (6.52 mmol) was added via syringe. The stirred mixture was allowed to warm to −40 °C, and 2.0 mL (32.15 mmol) of iodomethane was added. After stirring the reaction mixture at ambient temperature overnight, the reaction was worked up: 5 mL of water was added, volatiles were removed on a rotary evaporator, the residue was dissolved in ether, the organic solution was washed three times with water, the solution was dried with Na_2SO_4, ether was removed in vacuo, and the product was obtained by crystallization from a *n*-hexane solution: orange powder, mp 75−78 °C. Anal. Calcd for $C_{21}H_{20}FeO$: C, 73.27; H, 5.86. Found: C, 73.74; H, 5.88. IR (KBr): 3258 s ($\nu_{C\equiv C-H}$), 3110 w, 3093 w, 2967 m, 2932 w, 2913 w, 2828 w, 2116 w ($\nu_{C\equiv C}$), 1630 m, 1493 m, 1449 m, 1422 m, 1414 m, 1391 m, 1383 w, 1339 w, 1319 w, 1300 w, 1286 w, 1265 m, 1223 w, 1204 m, 1182 m, 1167 w, 1105 s, 1084 s, 1055 m, 1030 m, 1001 s, 984 m, 920 m, 904 w, 895 m, 866 m, 843 w, 833 w, 816 s, 760 s, 706 s, 688 m, 669 m, 630 m, 528 m, 501 s, 486 m, 466 m, 405 s cm^{-1}. MS (FAB): 345 (M^+ + H, 23%), 344 (M^+, 100%), 313 (M^+ − OCH_3, 41%), 306 (FcPhCOCH$_3$ + H, 19%); 305 (FcPhCOCH$_3$, 98%); 290 (FcPhCO, 57%) *m*/*e*. ^{1}H NMR ($CDCl_3$): 7.63 (2H, d, phenyl); 7.39 (3H, m, phenyl); 4.17 (2H, m, Cp); 4.14 (1H, m, Cp); 4.13 (5H, s, Cp); 4.08 (1H, m, Cp); 3.22 (2H, d, CH_2); 3.17 (3H, s, OCH_3); 2.01 (1H, t, C≡C−H) ppm. ^{13}C NMR ($CDCl_3$): 142.1, 127.7, 127.2, 127.1 (phenyl); 92.9 (C≡C); 80.8 (C(1) of butynol); 80.0 (C≡C); 71.2, 69.1, 68.6, 67.8, 67.6, 67.3 (Cp); 51.8 (OCH_3); 31.2 (CH_2) ppm.

1,5-Diferrocenyl-5-methoxy-1,5-diphenylpent-2-ynol (16). A Schlenk vessel charged with 1.00 g (2.91 mmol) of **15** and 150 mL of THF was cooled to −60 °C. A 1.25 mL portion of a 2.0 M pentane solution of *n*-butyllithium (3.04 mmol) was added, and the stirred mixture was allowed to warm to room temperature. A 0.84 g (2.91 mmol) sample of **1** was added in one portion, and the reaction mixture was stirred overnight. Workup: 5 mL of water was added, volatile materials were removed on a rotary evaporator, the residue was dissolved in ether, the organic solution was washed with aqueous $NaHCO_3$ and with water, the solution was dried with Na_2SO_4, solvents were removed in vacuo, and the residue was chromatographed on basic alumina with *n*-hexane/ether (v/v = 1:1) as eluent, affording 1.4 g of **16** in 78.5% yield: orange powder, mp 152−155 °C. Anal. Calcd for $C_{38}H_{34}Fe_2O_2$: C, 71.95; H, 5.40. Found: C, 71.72; H, 5.36. IR (KBr): 3548 s (ν_{OH}), 2089 m, 2932 w, 2853 m, 2822 w, 2203 w ($\nu_{C\equiv C}$), 1634 m, 1601 w, 1586 w, 1491 m, 1449 s, 1412 m, 1391 w, 1321 m, 1263 m, 1234 m, 1182 w, 1165 w, 1138 m, 1105 s, 1092 s, 1076 s, 1051 m, 1030 m, 1007 s, 943 w, 908 w, 825 s, 756 s, 677 s, 648 w, 609 w, 584 m, 519 s, 499 s, 459 m, 409 w cm^{-1}. MS (FAB): 636 (M^+ + 2H, 12%), 635 (M^+ + H, 44%), 634 (M^+, 100%), 633 (M^+ − H, 6%), 632 (M^+ − 2H, 12%), 617 (M^+ − OH, 3%), 603 (M^+ − OCH_3, 4%), 465 (M^+ − OH − OCH_3 − FeCp, 16%), 305 (FcPhCOCH$_3$, 82%); 290 (FcPhCO, 34%) *m*/*e*. ^{1}H NMR ($CDCl_3$): 7.70 (2H, d, phenyl); 7.42 (3H, m, phenyl); 7.34 (2H, d, phenyl); 7.18 (3H, m, phenyl); 4.20 (4H, m, Cp); 4.16 (5H, s, Cp); 4.14 (1H, m, Cp); 4.09 (5H, s, Cp); 4.08 (2H, m, Cp); 4.05 (1H, m, Cp); 3.41 (2H, s, CH_2); 3.27 (3H, s, OCH_3); 2.99 (1H, s, OH) ppm. ^{13}C NMR ($CDCl_3$): 144.6, 142.9, 127.8, 127.7, 127.3, 127.2, 127.16, 125.4 (phenyl); 97.7, 93.8 (C≡C); 93.4 (C(1) of pentynol); 85.7 (C(5) of pentynol); 81.9, 80.2, 71.2, 69.1, 68.8, 68.7, 68.4, 68.1, 67.9, 67.7, 67.1, 64.8 (Cp); 51.6 (OCH_3); 30.6 (CH_2) ppm.

1,5-Diferrocenyl-1,5-diphenylpentatrien-1-ylium Tetrafluoroborate (17a,b,c). A Schlenk tube was charged with 150 mL of ether and 0.16 g (0.25 mmol) of **16**. To this mixture, 38 mL of a 54% ethereal solution of HBF_4 (0.28 mmol) was added under stirring. Immediatly a purple precipitate was formed. After further stirring for 10 min, the product was filtered off under an atmosphere of Ar, washed with eher, and dried in vacuo, affording 0.12 g of **17a**,**b**,**c** in 71.3% yield: purple powder, mp >200 °C (dec). Anal. Calcd for $C_{37}H_{29}BF_4Fe_2$: C, 66.12; H, 4.35. Found: C, 66.00; H, 4.32. IR (KBr): 3108 w, 2925 w, 2101 s ($\nu_{C=C=C=C-C+}$), 1634 m, 1539 w, 1493 m, 1458 m, 1435 m, 1414 m, 1385 m, 1348 w, 1275 w, 1215 w, 1178 m, 1124 s, 1105 w, 926 m, 835 m, 773 w, 702 m, 675 w, 619 w, 592 w, 532 m, 482 m cm^{-1}. UV−vis (CH_2Cl_2; λ_{max}/ϵ): 384.5/11100, 541.0/13900, 940.5/10800 nm (Figure 9). MS (FAB): 585 (M^+ of cation, 100%) *m*/*e*. ^{1}H NMR (CD_2Cl_2): 7.79 (1H, t, phenyl); 7.52 (3H, m, phenyl); 7.44 (2H, t, phenyl); 7.34 (1H, s, phenyl); 7.32 (3H, m, phenyl); 6.14 (2H, m, Cp); 6.02 (1H, s, C_5H^+); 5.32 (2H, m, Cp); 5.09 (2H, m, Cp); 4.95 (2H, m, Cp); 4.70 (5H, s, Cp); 4.49 (5H, s, Cp) ppm. ^{13}C NMR (CD_2Cl_2): 166.1, 145.7 (C_5H^+); 139.5, 138.7, 133.2, 130.4, 129.7, 129.3, 128.8, 128.6 (phenyl); 110.8, 106.4, 100.4 (C_5H^+); 90.3, 86.2, 81.7, 77.9, 76.6, 73.4, 71.4 (Cp) ppm.

1,5-Diferrocenyl-1,5-diphenylpentatetraene (18) and 1,5-Diferrocenyl-1,5-diphenylpent-4-en-2-ynol (19). A Schlenk tube was charged with 50 mg (0.45 mmol) of potassium tertiary butoxide, 150 mL of dimethoxyethane, and 0.22 mL of a 2.0 M *n*-pentane solution of butyllithium (0.44 mmol). The mixture was cooled to −50 °C, and 0.2 g (0.30 mmol) of **17a**,**b**,**c** was added. Within 10 min the solution changed color to burgundy red; by TLC analysis a red product could be detected, indicating formation of **18**. Workup: the solution was filtered under an atmosphere of Ar through a short column of basic alumina, and volatiles were removed in vacuo. However, according to TLC analysis, the red product was converted to a yellow follow-up product during this process; unfortunately no experimental conditions could be found that allowed isolation of red C_5 cumulene **18**. Column chromatography on basic alumina with *n*-hexane/ether (v/v = 1:2) as eluent afforded 62 mg of **19** in 35.4% yield: orange crystals, mp 145−150 °C. Anal. Calcd for $C_{37}H_{30}Fe_2O$: C, 73.78; H, 5.02. Found: C, 73.69; H, 5.02. IR (KBr): 3567 m (ν_{OH}), 3087 m, 2963 w, 2199 w ($\nu_{C\equiv C}$), 1717 w, 1696 w, 1634 m, 1559 m, 1539 m, 1489 m, 1447 m, 1412 m, 1385 m, 1261 s, 1138 m, 1105 s, 1030 s, 906 m, 818 s, 771 m, 754 m, 715 m, 698 s, 588 w, 495 s cm^{-1}. MS (FAB): 604 (M^+ + 2H, 11%), 603 (M^+ + H, 46%), 602 (M^+, 100%), 600 (M^+ − 2H, 14%), 586 (M^+ + H − OH, 27%), 585 (M^+ − OH, 56%), 465 (M^+ + H − OH − FeCp, 25%), 464 (M^+ − OH − FeCp, 48%), 463 (M^+ − H − OH − FeCp, 10%), 400 (M^+ − OH − Fc, 10%), 399 (M^+ − H − OH − Fc, 25%), 291 (FcPhCOH), 14%), 290 (FcPhCO, 22%) *m*/*e*. ^{1}H NMR (CD_2Cl_2): 7.54 (2H, m, phenyl); 7.49 (2H, m, phenyl); 7.40 (3H, m, phenyl); 7.24 (3H, m, phenyl); 6.18 (1H, s, C═CH); 4.36 (1H, m, Cp); 4.32 (2H, m, Cp); 4.19 (2H, m, Cp); 4.16 (5H, s, Cp); 4.12 (5H, s, Cp); 4.08 (2H, m, Cp); 3.96 (1H, m, Cp); 2.95 (1H, s, OH) ppm. ^{13}C NMR (CD_2Cl_2): 152.8 (═CH); 144.2, 139.6, 129.2, 128.1, 127.9, 127.7, 127.3, 125.4 (phenyl); 103.0 (C═CH); 97.3, 95.5 (C°C); 84.5, 84.3 (Cp); 71.8 (COH); 69.7, 69.1, 68.8, 68.5, 68.1, 67.9, 67.5, 67.1, 64.9 ppm. Single crystals were obtained from a dichloromethane solution (Figure 7).

1.6-Diferrocenyl-1,6-diphenylhexapentaene (22a,b). A Schlenk flask was charged with 0.5 g (1.51 mmol) of **9** and 150 mL of THF. After the mixture was cooled to − 60 °C, 1.15 mL of a 2.0 M pentane solution of *n*-butyllithium (3.30 mmol) was added, and the stirred mixture was allowed to warm to ambient temperature. A red solution was formed, indicating formation of lithiated **20**. The solution was refluxed under an atmosphere of Ar, and a gradual color change from red to dark purple was observed, indicating dimerization of **21a**,**b**; by TLC analysis minor amounts of the purple product **22a**,**b** were detected besides ferrocenylphenylpropynol (hydrolyzed **21a**,**b**).

After refluxing the solution for 12 h, the mixture was worked up, although reaction was not complete; longer reaction periods led to formation of a black insoluble tar. The mixture was filtered through a short column of basic alumina, volatile materials were removed on a rotary evaporator, and column chromatography on basic alumina using *n*-hexane/ether (v/v = 1:5) as eluent afforded 25 mg of **22a**,**b** in 5.6% yield (due to decomposition/immobilization of the product on the stationary phase, the chromatography has to be done as quickly as possible and no better yield could be obtained): purple powder, mp >244 °C (dec). Anal. Calcd for $C_{38}H_{28}Fe_2$: C, 76.54; H, 4.73. Found: C, 76.47; H, 4.76. IR (KBr): 3089 w, 2925 w, 1647 m, 1560 w, 1533 w, 1489 m, 1458 m, 1377 w, 1286 m, 1256 s, 1211 m, 1150 s, 1105 m, 1057 w, 1041 w, 1028 m, 1001 m, 943 w, 820 s, 762 m, 694 s, 667 m, 586 w, 501 s, 486 m, 457 m cm^{-1}. Raman IR: 1962 s ($\nu_{C=C=C=C=C}$), 1569 w, 1485 w, 1230 w, 762 w, 658 w cm^{-1}. UV−vis (CH_2Cl_2; λ_{max}/ϵ): 380.0/5790, 478.5/9240, 512.0/9610, 618.0/4410 nm (Figure 8). MS (FAB): 597 (M^+ + H, 13%), 596 (M^+, 21%), 595 (M^+ − H, 4%), 594 (M^+ − 2H, 4%), 411 (M^+ − Fc, 6%), 307 (nitrobenzyl alcohol, matrix, 100%), 274 (FcPhC, 15%) *m*/*e*. ^{1}H NMR (CD_2Cl_2): 7.77 (4H, d, phenyl); 7.37 (6H, m, phenyl); 4.82 (4H, m, Cp); 4.55 (4H, m, Cp); 4.16 (10H, s, Cp) ppm. ^{13}C NMR (CD_2Cl_2): 144.1 (C=C=C=C=C=C); 138.9, 128.8, 128.3 (phenyl); 126.9, 122.8 (C=C=C=C=C=C); 84.3, 70.7, 69.7, 67.4 (Cp) ppm.

1-Ferrocenyl-1-phenylpenta-2,4-diynol (24) and 1,6-Diferrocenyl-1,6-diphenylhexa-2,4-diyn-1,6-diol (25). A Schlenk round-bottom flask charged with 150 mL of THF and 0.34 g (1.75 mmol) of bis(trimethylsilyl)butadiyne (**23**) was cooled to −60 °C. A 1.80 mL portion of a 2.0 M pentane solution of *n*-butyllithium (3.60 mmol) was added via syringe, and the stirred mixture was allowed to warm to room temperature. A 1.0 g (3.45 mmol) sample of **1** was added in one portion under protection from air, and the reaction was stirred for 60 h at ambient temperature. Workup: 5 mL of water was added, volatiles were removed on a rotary evaporator, the yellow residue was dissolved in dichloromethane, the organic solution was washed three times with water and dried with Na_2SO_4, solvent was removed in vacuo, and the crude product mixture was chromatographed on basic alumina with *n*-hexane/ether (v/v = 1:1) as eluent, affording 0.2 g of **24** in 34.5% yield and **25** in 14.6% yield, respectively.

Data for **24**: yellow powder, mp 87−90 °C. Anal. Calcd for $C_{21}H_{16}FeO$: C, 74.14; H, 4.74. Found: C, 74.06; H, 4.71. IR (KBr): 3531 m (ν_{OH}), 3268 s ($\nu_{C\equiv C-H}$), 3025 w, 2062 w ($\nu_{C\equiv C-C\equiv C}$), 1659 w, 1599 w, 1489 m, 1449 s, 1408 m, 1391 m, 1377 m, 1323 s, 1288 m, 1236 m, 1215 w, 1175 m, 1159 w, 1138 s, 1103 m, 1078 w, 1063 m, 1045 m, 1030 m, 1001 s, 930 s, 895 w, 864 m, 856 m, 825 s, 750 s, 696 s, 677 m, 659 s, 646 s, 598 w, 584 m, 505 s, 495 s, 486 s, 480 s, 426 m cm^{-1}. MS (FAB): 341 (M^+ + H, 20%), 340 (M^+, 100%), 323 (M^+ − OH, 20%) *m*/*e*. ^{1}H NMR ($CDCl_3$): 7.54 (2H, d, phenyl); 7.31 (3H, m, phenyl); 4.44 (1H, m, Cp); 4.33 (5H, s, Cp); 4.30 (1H, m, Cp); 4.26 (1H, m, Cp); 4.18 (1H, m, Cp); 3.20 (1H, s, OH); 2.33 (1H, s, C≡C−H) ppm. ^{13}C NMR ($CDCl_3$): 142.7, 128.1, 127.9, 125.4 (phenyl); 95.9, 78.5, 71.7 (C−C≡C−C≡C−H); 69.5, 69.0, 68.4, 68.3, 67.5, 65.0 (Cp) ppm.

Data for **25**: yellow powder, mp 143−146 °C. Anal. Calcd for $C_{38}H_{30}Fe_2O_2$: C, 72.41; H, 4.80. Found: C, 72.32; H, 4.79. IR (KBr): 3536 s (ν_{OH}), 2925 s, 2853 m, 1742 m, 1634 m, 1491 w, 1456 m, 1385 m, 1373 m, 1296 m, 1279 s, 1263 m, 1234 m, 1178 s, 1144 s, 1105 s, 1051 s, 1041 s, 1020 s, 914 m, 881 w, 825 s, 767 m, 702 s, 683 w, 659 w, 586 w, 532 w, 492 m, 455 w cm^{-1}. MS (FAB): 632 (M^+ + 2H, 11%), 631 (M^+ + H, 46%), 630 (M^+, 100%), 628 (M^+ − 2H, 13%), 614 (M^+ − OH + H, 14%), 613 (M^+ − OH, 31%) *m*/*e*. ^{1}H NMR ($CDCl_3$): 7.55 (4H, d, phenyl); 7.30 (6H, m, phenyl); 4.46 (2H, m, Cp); 4.34 (10H, s, Cp); 4.31 (2H, m, Cp); 4.26 (2H, m, Cp); 4.18 (2H, m, Cp); 3.21 (2H, s, OH) ppm. ^{13}C NMR ($CDCl_3$): 142.9, 128.1, 127.9, 125.5 (phenyl); 96.1, 82.8, 71.9 (C−C≡C−C≡C−C); 69.1, 68.5, 68.45, 65.1 (Cp) ppm.

3-Ferrocenyliodo-3-methoxy-3-phenylpropyne (26). A Schlenk tube charged with 150 mL of THF and 1.0 g of **9** was cooled to −60 °C. Addition of 1.60 mL of a 2.0 M *n*-pentane solution of *n*-butyllithium (3.20 mmol) and warming to room temperature effected lithiation of **9**. Under protection from air, 0.77 g (3.03 mmol) of I_2 was added, and stirring was continued for 18 h. Workup: 5 mL of water was added, volatiles were removed in vacuo, the residue was dissolved in ether, the organic solution was washed with aqueous $NaHCO_3$ and with water, the solution was dried with Na_2SO_4, solvents were removed in vacuo, and chromatography of the crude product on basic alumina with *n*-hexane/ether (v/v = 2:1) afforded 0.77 g of **26** in 55.7% yield: yellow powder, mp 120−123 °C. Anal. Calcd for $C_{20}H_{17}FeIO$: C, 52.67; H, 3.76. Found: C, 52.71; H, 3.78. IR (KBr): 3108 w, 3091 w, 3058 w, 2950 w, 2929 w, 2896 m, 2822 m, 2172 w ($\nu_{C\equiv C}$), 1767 w, 1645 m, 1599 m, 1489 m, 1447 s, 1410 w, 1393 m, 1312 w, 1242 m, 1221 m, 1190 m, 1167 m, 1101 s, 1080 s, 1061 m, 1049 m, 1030 s, 1005 m, 958 m, 947 m, 914 w, 872 w, 848 m, 821 s, 756 s, 710 s, 696 m, 673 m, 627 m, 551 w, 520 m, 505 s, 486 s, 445 m, 410 w cm^{-1}. MS (FAB): 457 (M^+ + H, 22%), 456 (M^+, 100%), 330 (M^+ + H − I, 28%), 241 (M^+ + H − I − C≡C − Cp, 19%), 178 (CpPhCC≡C + H, 19%), 57 (Fe + H, 27%) *m*/*e*. ^{1}H NMR ($CDCl_3$): 7.61 (2H, d, phenyl); 7.36 (3H, m, phenyl); 4.45 (1H, m, Cp); 4.15 (1H, m, Cp); 4.13 (5H, s, Cp); 4.05 (1H, m, Cp); 3.93 (1H, m, Cp); 3.28 (3H, s, OCH_3) ppm. ^{13}C NMR ($CDCl_3$): 140.9, 127.9, 126.8 (phenyl); 94.5, 94.1 (C≡C); 80.6 (C(1) of propyne); 69.3, 67.9, 67.86, 67.3, 66.9 (Cp); 53.0 (OCH_3) ppm.

1,7-Diferrocenyl-1,7-dimethoxy-1,7-diphenylhepta-2,4-diyne (27) and 1,6-Diferrocenyl-1,6-dimethoxy-1,6-diphenylhexa-2,4-diyne (28). A Schlenk vessel charged with 100 mL of THF and 0.14 g (0.41 mmol) of **15** was cooled to −60 °C. Then 0.31 mL of a 1.4 M ethereal solution of methyllithium (0.43 mmol) was added via syringe, and the mixture was allowed to warm to room temperature. After cooling to −60 °C, 0.24 g (1.17 mmol) of $CuBr\cdot(H_3C)_2S$ was added and the mixture was stirred and allowed to warm to room temperature. Volatile materials were removed on a vacuum line in an oil pump vacuum until approximately 5 mL of material was left over, and 30 mL of dry, deoxygenated pyridine was added, followed by 0.19 g (0.42 mmol) of **26**. The mixture was refluxed for 1 h and worked up: solvents and other volatiles were removed in vacuo, the residue was dissolved in dichloromethane, the organic solution was filtered and washed three times with water, the solution was dried with Na_2SO_4, solvent was removed in vacuo, and chromatography on basic alumina with *n*-hexane/ether (v/v = 5:1) as eluent afforded 80 mg of **27** in 28.6% yield and the homocoupled product **28** in 21.8% yield, respectively.

Data for **27**: yellow powder, mp 75−80 °C. Anal. Calcd for $C_{41}H_{36}Fe_2O_2$: C, 73.23; H, 5.40. Found: C, 73.15; H, 5.38. IR (KBr): 3094 w, 2934 w, 2900 w, 2824 w, 2171 w ($\nu_{C\equiv C}$), 1634 m, 1599 m, 1489 m, 1445 m, 1412 s, 1319 w, 1312 w, 1261 w, 1240 w, 1219 w, 1186 m, 1173 m, 1107 s, 1049 s, 1030 m, 1018 m, 1003 s, 955 m, 941 m, 820 m, 754 m, 700 s, 683 s, 592 w, 495 s, 486 s, 447 m cm^{-1}. MS (FAB): 673 (M^+ + H, 32%), 672 (M^+, 68%), 670 (M^+ − 2H, 8%), 641 (M^+ − OCH_3, 8%), 489 (M^+ − 2OCH_3 − FeCp, 12%), 305 ($CpPhC_5CH_2CPh$ + H, 100%) *m*/*e*. ^{1}H NMR ($CDCl_3$): 7.64 (2H, d, phenyl); 7.58 (2H, m, phenyl); 7.40 (3H, m, phenyl); 7.33 (3H, m, phenyl); 4.43 (1H, m, Cp); 4.20 (2H, m, Cp); 4.18 (5H, s, Cp); 4.14 (2H, m, Cp); 4.11 (5H, s, Cp); 4.10 (1H, m, Cp); 4.03 (1H, m, Cp); 3.89 (1H, m, Cp); 3.37 (2H, d, CH_2); 3.24 (3H, s, OCH_3); 3.19 (3H, s, OCH_3) ppm. ^{13}C NMR ($CDCl_3$): 140.9, 127.9, 126.8 (phenyl); 94.5, 94.1 (C≡C); 80.6 (C(1) of propyne); 69.3, 67.9, 67.86, 67.3, 66.9 (Cp); 53.0 (OCH_3) ppm.

Data for **28**: orange powder, mp 111−113 °C. Anal. Calcd for $C_{40}H_{34}Fe_2O_2$: C, 72.97; H, 5.21. Found: C, 72.87; H, 5.17. IR (KBr): 3093 m, 3056 w, 3019 w, 2203 m ($\nu_{C\equiv C}$), 1958 w, 1643 m, 1597 m, 1584 m, 1574 m, 1489 m, 1460 w, 1447 s, 1410 w, 1393 w, 1379 w, 1331 m, 1267 m, 1234 m, 1180 w,

1159 m, 1138 m, 1105 s, 1074 w, 1053 m, 1043 m, 1032 m, 1005 s, 943 m, 906 m, 866 w, 835 s, 821 s, 775 m, 758 s, 715 m, 700 s, 677 m, 652 m, 582 w, 519 s, 493 s, 457 m, 434 w, 407 w cm^{-1}. MS (FAB): 659 (M^+ + H, 12%), 658 (M^+, 23%), 460 (M^+ − Ph − FeCp, 15%), 307 (nitrobenzyl alcohol, matrix, 100%), 290 (FcPhCO, 19%) *m/e*. ^{1}H NMR ($CDCl_3$): 7.66 (4H, d, phenyl); 7.39 (6H, m, phenyl); 4.20 (10H, s, Cp); 4.18 (2H, m, Cp); 4.08 (2H, m, Cp); 3.98 (2H, m, Cp); 3.35 (6H, s, OCH_3) ppm. ^{13}C NMR ($CDCl_3$): 140.7, 128.1, 128.08, 126.8 (phenyl); 93.6, 79.9 (C≡C); 79.8 (C(1) and C(6) of hexadiyne); 71.9, 69.5, 68.1, 68.07, 67.4, 66.9 (Cp); 53.2 (OCH_3) ppm.

1,7-Diferrocenyl-1,7-diphenylheptapentaen-1-ylium Tetrafluoroborate (29a,b,c,d). A Schlenk tube was charged with 10 mL of dichloromethane and with 90 mg (0.13 mmol) of **27**. To this solution was added 21 mL of a 54% ethereal solution of HBF_4 (0.15 mmol) under an atmosphere of Ar, followed by 60 mL of *n*-hexane. Immediatly a dark green precipitate was formed. The suspension was stirred for 10 min, the precipitated product was filtered off under Ar, and the product was washed with three portions of *n*-hexane and dried in vacuo, affording 90 mg of **29a**,**b**,**c**,**d** in 95.5% yield: dark green powder, mp >260 °C (dec). Anal. Calcd for $C_{39}H_{29}BF_4Fe_2$: C, 67.29; H, 4.20. Found: C, 67.42; H, 4.23. IR (KBr): 3104 w, 2963 w, 2049 s ($\nu_{C=C=C=C=C-C+}$), 1638 w, 1576 w, 1530 m, 1493 m, 1437 s, 1412 m, 1383 m, 1325 m, 1300 m, 1234 s, 1180 m, 1140 m, 1107 s, 1048 s, 1053 s, 1001 m, 821 m, 769 m, 721 m, 700 s, 657 w, 619 w, 588 w, 486 s cm^{-1}. UV−vis (CH_2Cl_2; λ_{max}/ϵ): 342.5/15167, 465.0/8047, 629.0/6762, 1071.5/8040 nm (Figure 9). MS (FAB): 609 (M^+ of cation, 29%), 307 (nitrobenzyl alcohol, matrix, 100%) *m/e*. ^{1}H NMR and ^{13}C NMR: only very broad and noninformative spectra could be obtained (see text of article).

Acknowledgment. B.B. and W.S. thank the Austrian Science Fund FWF (P13073-PHY) for support of this research. P.Z. gratefully acknowledges financial support from the University of Siena (PAR 2003).

Supporting Information Available: Crystallographic and electrochemical procedures and data. This material is available free of charge via the Internet at http://pubs.acs.org.

OM034233L